

ROC curve analysis for functional markers

Ana M. Bianco^a, Graciela Boente^b and Juan Carlos Pardo-Fernández^c

^a Instituto de Cálculo, Facultad de Ciencias Exactas y Naturales,

Universidad de Buenos Aires and CONICET, Argentina

^a email: abianco@dm.uba.ar

^b Departamento de Matemáticas and Instituto de Cálculo, Facultad de Ciencias Exactas y Naturales,

Universidad de Buenos Aires and CONICET, Argentina

^c Centro de Investigación e Tecnoloxía Matemática de Galicia (CITMAga) and

Departamento de Estatística e Investigación Operativa, Universidade de Vigo, Spain

Abstract

Functional markers have become a frequent tool in medical diagnosis. In this paper, we aim to define an index allowing to discriminate between populations when the observations are functional data belonging to a Hilbert space. We discuss some of the problems arising when estimating optimal directions defined to maximize the area under the curve of a projection index and we construct the corresponding ROC curve. We also go one step further and consider the case of possibly different covariance operators, for which we recommend a quadratic discrimination rule. Consistency results are derived for both linear and quadratic indexes under mild conditions. The results of our numerical experiments allow to see the advantages of the quadratic rule when the populations have different covariance operators. We also illustrate the considered methods on a real data set on cardiotoxicity related to therapies on breast cancer patients.

Keywords: Consistency; Discriminating index; Functional data; Optimal directions; ROC curve.

1 Introduction

In applied sciences, there is a permanent search for better and better tools of diagnosis and screening of different diseases. A key-point is the evaluation of the performance of such developments. The Receiver Operating Characteristic curve (ROC curve) is a very well-accepted graphical technique to assess the accuracy of a diagnostic test based on a continuous marker. The use of ROC curves is extensive in medical and pharmacological investigations, but they are also employed in completely different scenarios, such as for the evaluation of a machine learning process, see [Krzanowski and Hand \(2009\)](#) where more applications can be found.

For the sole purpose of introducing the concepts related to ROC curves, we will focus on medical diagnosis, where there are two groups, corresponding to diseased and healthy populations, and the aim is to classify a new subject in one of these groups according to the outcome of a continuous biomarker. In this context, two essential concepts appear concerning the errors one can make: the *sensitivity*, related to the ability of correctly detecting diseased people, and the *specificity*, that involves the skill of correctly assigning a subject to the healthy group. Thus, a ROC curve for a test based on a continuous marker is a graphical representation of the *sensitivity* against the complementary of the *specificity* (that is, $1 - \text{specificity}$) computed from the classification rule that assigns a subject to the diseased group if the biomarker is greater than a critical value c and to the healthy group, otherwise, as the threshold c varies.

In order to compact the information about the discriminatory performance of the diagnostic test several summary indexes were introduced. The classification accuracy is frequently measured through the area under the curve (AUC), which can be interpreted as the average sensitivity for all specificity values. The Youden index, YI, is another global measure that is extensively used in the literature and corresponds to the maximum difference between the ROC curve and the identity function. Estimation and inference methods regarding ROC curve and related summary measures are very well-studied in the univariate setting. [Pepe \(2003\)](#) and [Zhou et al. \(2011\)](#) provide a comprehensive review concerning both theoretical and practical aspects of ROC curves based on univariate markers.

For some diseases, it is necessary to combine several biomarkers in order to get a diagnosis tool that improves the performance of each single marker on its own. In such cases, a global diagnostic measure is desirable to achieve a better classification rule. [Pérez-Fernández \(2020\)](#) reviews some proposals given to summarize the joint information provided by several biomarkers, including methods based on linear and quadratic discrimination rules.

In recent years with the evolution of biomedical technology, data with more and more complex structure are collected. This is the case of functional data that consist of curves varying over time or any other continuum and thus, valued in an infinite-dimensional space, usually a metric or semi-metric, and in some cases, a Hilbert space. Henceforth, we will assume that the functional data are measured over time. In fact, functional markers have been increasingly used in clinical studies to diagnose diseases. To summarize the curves in a univariate biomarker usual practices are to consider the maximum or minimum values, the time to the maximum or the integral of the curve over the time range. However, specifically designed techniques should be employed to analyse this kind of data in order to take advantage of their potential and, as extensively discussed, the infinite-dimensional structure should be taken into account when considering any estimation procedure, see [Wang et al. \(2016\)](#). For an overview on functional data analysis we refer among others to [Ramsay and Silverman \(2005\)](#), [Ferraty and Vieu \(2006\)](#), [Horváth and Kokoszka \(2012\)](#) and [Hsing and Eubank \(2015\)](#).

Our contribution is oriented to situations such as the one described in [Section 6](#), where we address a study on breast cancer patients with high levels of the protein human epidermal growth factor receptor 2 (HER2). These women have a better response to drugs that target the HER2 protein, but this kind of therapies may have side effects such as cardiotoxicity. In order to prevent therapy-related cardiac dysfunction (CTRCD), it is recommended to follow-up the appearance of CTRCD through cardiac imaging tests such as the Tissue Doppler Imaging (TDI), an echocardiographic technique that reflects the myocardial motion. TDI is processed so as to obtain a functional datum used to study the heart status. The aim is to evaluate the performance of this functional biomarker, which is displayed in [Figure 1](#), to distinguish between patients with CTRCD from those who do not suffer from this condition. Gray curves

correspond to patients without CTRCD (CTRCD= 0) and aquamarine ones to women with CTRCD (CTRCD= 1). At a first glance, the two groups look different since the cycles of patients without CTRCD are more spread, while the data of women that experienced CTRCD are more concentrated in the central area. Besides, the means of the two groups are similar, except for cycle values between 0.4 and 0.8. It is worth mentioning that the data set is available at [Piñeiro-Lamas et al. \(2023\)](#), where a thorough description is given.

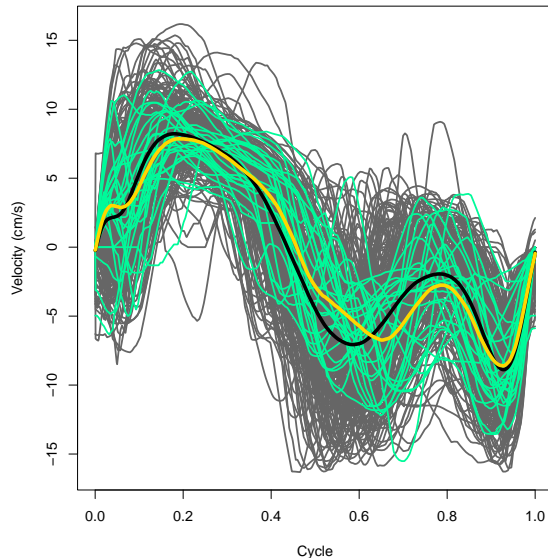


Figure 1: Cardiotoxicity data. Cycles of 270 patients during the follow-up. The cycles of patients with CTRCD= 0 are displayed as gray lines, while those with CTRCD= 1 are represented in aquamarine. The lines in black and gold correspond to the mean of CTRCD= 0 and CTRCD= 1, respectively.

Functional data, that become more frequent every day in clinical research, pose different challenges to Statistics, in particular, to ROC curve estimation. In this direction, some developments were done to extend the existing methodology to the functional setting. For instance, proposals for the induced ROC considering a univariate marker and a functional covariate are considered by [Inácio et al. \(2012\)](#) and [Inácio de Carvalho et al. \(2016\)](#). However, in some situations, the biomarker itself is a functional data usually discretely recorded. This is often the case in longitudinal studies and we refer to [Liu and Wu \(2003\)](#) and [Liu et al. \(2005\)](#), who propose a generalized mixed model to predict the condition (healthy or diseased) based on the observed values of the biomarker. [Haben et al. \(2019\)](#) consider a dynamic scoring prediction

rule and then several extensions of the ROC curve are introduced. When the biomarker is discretely recorded with some possible noise, smoothing techniques, such as smoothing splines and kernel smoothing, can be employed, see [Wang et al. \(2016\)](#).

In the context of functional biomarker, [Estévez-Pérez and Vieu \(2021\)](#) define a functional version of the ROC curve by properly ranking the sample of functional data via the projection over a selected subset \mathcal{E} of the functional space indexed by a real number $\theta \in [0, 1]$. The functional ROC curve is then defined as the ROC of the projections over \mathcal{E} . As mentioned therein, their proposal is appropriate when differences between healthy and diseased individuals arise in their mean, but not on the covariances. Later, [Jang and Manatunga \(2022\)](#) propose a wide class of features to summarize the functional biomarker into an univariate one, including an integral-type that can also be viewed as the inner L^2 -product between the functional data and the constant function that corresponds to the average value of the functional marker. Among these features, they consider the average velocity and average acceleration as well as the maximum and minimum of the biomarker curve mentioned above. The ROC curves and the corresponding AUC are then constructed using the summary functional and the smoothed trajectories.

In this paper, we follow a unifying approach. We first review in [Section 2](#) the basic notions related to ROC curves and the situation of multivariate biomarkers, where methods based on searching for linear combinations maximizing the AUC were given. Later on, in [Section 3](#) we adapt these revisited ideas to the functional framework assuming that the trajectories belong to a Hilbert space and we discuss the issues involved in the estimation of the optimal directions. We also go one step forward, by considering the case of possibly different covariance operators. [Section 4](#) is devoted to the study of asymptotic properties, such as the uniform consistency of the proposed ROC curve estimators and the strong consistency of the related estimators of the AUC and the Youden index. In [Section 5](#) a thorough numerical experiment is performed, while in [Section 6](#) the analysis of the real data set mentioned above illustrates the application of the studied procedures. Some final comments are provided in [Section 7](#). Proofs are relegated to the Appendix.

2 Preliminaries

2.1 Basic notions and multivariate biomarkers

We begin by introducing basic concepts related to ROC curves in the simple case of a univariate biomarker. Assume that Y is a continuous biomarker and let c be a threshold value. Thus, we consider the classification rule that assigns a subject to the diseased group when $Y \geq c$ and to the healthy one, otherwise. Moreover, denote Y_D the marker in the diseased population and F_D its distribution, while Y_H and F_H stand for the marker and its distribution in the healthy population. As usual in this context, the populations are assumed to be independent. Our interest focuses on the evolution of the pairs $\{(1 - F_H(c), 1 - F_D(c))\}$ as the threshold $c \in \mathbb{R}$ varies. This leads to the usual ROC curve formula given by $\text{ROC}(p) = 1 - F_D\{F_H^{-1}(1 - p)\}$, $p \in (0, 1)$.

An extensively used model is the binormal one, that assumes that in both populations the marker is normally distributed, i.e., $F_j \sim N(\mu_j, \sigma_j)$, for $j = D, H$. In this case, the distributions are characterized by the means μ_j and the standard deviations σ_j , $j = D, H$, leading to $\text{ROC}(p) = \Phi\{(\mu_H - \mu_D)/\sigma_D + \sigma_H\Phi^{-1}(p)/\sigma_D\}$, where Φ stands for the cumulative distribution function of a standard normal variable.

In order to have a global measure of the accuracy of the test, different indexes have been introduced. The area under the ROC curve (AUC) is the most popular and is defined as $\text{AUC} = \int_0^1 \text{ROC}(p) dp$. Straightforward calculus enables to prove that $\text{AUC} = \mathbb{P}(Y_D > Y_H)$ and this is why values of AUC near to 1 are related to high diagnostic accuracy of the biomarker. The Youden index, YI, is also very well known. It measures the proximity of the ROC curve to the identity function, thinking of the identity as the ROC of useless marker, and is defined as $\text{YI} = \max_{0 < p < 1} \{\text{ROC}(p) - p\}$. It is worth mentioning that when Y_D is stochastically greater than Y_H , then $\text{ROC}(p) \geq p$, so the area under the curve is greater or equal than 0.5 and the Youden index is non-negative.

Now, let us consider the multivariate case where $\mathbf{x} \in \mathbb{R}^k$ is the multivariate biomarker used

for the diagnostic of a given disease. From now on, $\mathbf{x}_D \sim F_D$ and $\mathbf{x}_H \sim F_H$ stand for the independent biomarkers over the diseased and healthy populations, respectively. A well-known discrimination rule is the linear one, which intends to project the data over a given direction chosen to differentiate both groups. For a given $\boldsymbol{\beta} \in \mathbb{R}^k$ denote $Y_{j,\boldsymbol{\beta}} = \boldsymbol{\beta}^\top \mathbf{x}_j$, for $j = D, H$, and let $F_{j,\boldsymbol{\beta}}$ their respective distribution functions. Then, a ROC curve can be constructed for each fixed $\boldsymbol{\beta} \neq \mathbf{0}_k$ as $\text{ROC}_\beta(p) = 1 - F_{D,\boldsymbol{\beta}}\{F_{H,\boldsymbol{\beta}}^{-1}(1-p)\}$, $p \in (0, 1)$. ROC_β allows to evaluate the capability of the projected biomarker to distinguish between the two groups. Among others, [Ma and Huang \(2005\)](#) and [Pepe et al. \(2006\)](#) provide methods to choose the best direction by means of the area under the curve $\text{AUC}(\boldsymbol{\beta}) = \int_0^1 \text{ROC}_\beta(p) dp = \mathbb{P}(Y_{D,\boldsymbol{\beta}} > Y_{H,\boldsymbol{\beta}})$. In [Section 2.2](#), we review the construction of the optimal direction on a population level for normally distributed biomarkers, to understand how these ideas can be extended to the functional case, as presented in [Section 3.1](#).

2.2 The binormal case

The binormal model has been extensively considered for univariate biomarkers as a way to supply a simple parametric approach to ROC curves estimation. Hence, if the practitioner suspects that this model gives a suitable approximation, they can choose the threshold constants according to that belief, providing a semiparametric framework that will indeed keep consistency under the suspected model. In the multivariate setting, the binormal model also provides a simple expression for both the $\text{ROC}_\beta(p)$ and the $\text{AUC}(\boldsymbol{\beta})$.

Let us assume that $\mathbf{x}_j \sim N(\boldsymbol{\mu}_j, \boldsymbol{\Sigma}_j)$, hence $Y_{j,\boldsymbol{\beta}} \sim N(\boldsymbol{\beta}^\top \boldsymbol{\mu}_j, \boldsymbol{\beta}^\top \boldsymbol{\Sigma}_j \boldsymbol{\beta})$. Denote z_p the value such that $\Phi(z_p) = 1 - p$. As it is well known, in such framework, the quantile and distribution functions of $Y_{H,\boldsymbol{\beta}}$ and $Y_{D,\boldsymbol{\beta}}$, respectively have an explicit expression given by

$$F_{H,\boldsymbol{\beta}}^{-1}(1-p) = \boldsymbol{\beta}^\top \boldsymbol{\mu}_H + (\boldsymbol{\beta}^\top \boldsymbol{\Sigma}_H \boldsymbol{\beta})^{1/2} z_p \quad \text{and} \quad F_{D,\boldsymbol{\beta}}(u) = \Phi \left\{ \frac{u - \boldsymbol{\beta}^\top \boldsymbol{\mu}_D}{(\boldsymbol{\beta}^\top \boldsymbol{\Sigma}_D \boldsymbol{\beta})^{1/2}} \right\},$$

which allow to express the related ROC_β curve using the cumulative standard normal distribu-

tion as

$$\text{ROC}_{\beta}(p) = 1 - F_{D,\beta} \left\{ \boldsymbol{\beta}^{\top} \boldsymbol{\mu}_H + (\boldsymbol{\beta}^{\top} \boldsymbol{\Sigma}_H \boldsymbol{\beta})^{1/2} z_p \right\} = 1 - \Phi \left\{ \frac{\boldsymbol{\beta}^{\top} (\boldsymbol{\mu}_H - \boldsymbol{\mu}_D) + (\boldsymbol{\beta}^{\top} \boldsymbol{\Sigma}_H \boldsymbol{\beta})^{1/2} z_p}{(\boldsymbol{\beta}^{\top} \boldsymbol{\Sigma}_D \boldsymbol{\beta})^{1/2}} \right\}.$$

Furthermore, taking into account that $Y_{D,\beta} - Y_{H,\beta} \sim N(\mu_{\beta}, \sigma_{\beta}^2)$, with $\mu_{\beta} = \boldsymbol{\beta}^{\top} (\boldsymbol{\mu}_D - \boldsymbol{\mu}_H)$ and $\sigma_{\beta}^2 = \boldsymbol{\beta}^{\top} (\boldsymbol{\Sigma}_D + \boldsymbol{\Sigma}_H) \boldsymbol{\beta}$, an explicit expression may also be given for the $\text{AUC}(\boldsymbol{\beta})$ as

$$\text{AUC}(\boldsymbol{\beta}) = \mathbb{P}(Y_{D,\beta} - Y_{H,\beta} > 0) = \Phi \left[\frac{\boldsymbol{\beta}^{\top} (\boldsymbol{\mu}_D - \boldsymbol{\mu}_H)}{\{\boldsymbol{\beta}^{\top} (\boldsymbol{\Sigma}_D + \boldsymbol{\Sigma}_H) \boldsymbol{\beta}\}^{1/2}} \right].$$

Note that when $\boldsymbol{\mu}_D = \boldsymbol{\mu}_H$ the $\text{AUC}(\boldsymbol{\beta})$ equals 1/2 for any $\boldsymbol{\beta}$ and the problem of maximizing $\text{AUC}(\boldsymbol{\beta})$ is vacuous. Furthermore, if $\boldsymbol{\Sigma}_H = \boldsymbol{\Sigma}_D$, then, the function $\text{ROC}_{\beta}(p)$ is constant and equal to the identity function, since both populations cannot be distinguished.

Ma and Huang (2007) propose to estimate $\boldsymbol{\beta}$ as the value maximizing a smooth estimator, $\widehat{\text{AUC}}(\boldsymbol{\beta})$, of $\text{AUC}(\boldsymbol{\beta})$. Taking into account that the area under the curve and ROC_{β} remain unchanged if $\boldsymbol{\beta}$ is multiplied by a positive constant, Ma and Huang (2007) suggest to maximize $\widehat{\text{AUC}}(\boldsymbol{\beta})$ over the values $\boldsymbol{\beta}$ such that the first coordinate equals 1. When constructing the smooth estimator $\widehat{\text{AUC}}(\boldsymbol{\beta})$ the indicator function is approximated by the sigmoid function.

It is clear that the population counterparts of the estimators defined in Ma and Huang (2007) correspond to the value $\boldsymbol{\beta}$ maximizing $\text{AUC}(\boldsymbol{\beta})$ over the directions with its first component equal to 1, or equivalently to the maximizer of

$$L(\boldsymbol{\beta}) = \frac{\boldsymbol{\beta}^{\top} (\boldsymbol{\mu}_D - \boldsymbol{\mu}_H)}{\{\boldsymbol{\beta}^{\top} (\boldsymbol{\Sigma}_D + \boldsymbol{\Sigma}_H) \boldsymbol{\beta}\}^{1/2}}. \quad (1)$$

The Cauchy–Schwartz inequality implies that any scalar multiple of $\boldsymbol{\beta}_0 = (\boldsymbol{\Sigma}_D + \boldsymbol{\Sigma}_H)^{-1} (\boldsymbol{\mu}_D - \boldsymbol{\mu}_H)$ maximizes $|L(\boldsymbol{\beta})|$, so $\boldsymbol{\beta}_0$ (and any its positive multiples) maximizes $\text{AUC}(\boldsymbol{\beta})$ leading to

$$\max_{\boldsymbol{\beta}} \text{AUC}(\boldsymbol{\beta}) = \text{AUC}(\boldsymbol{\beta}_0) = \Phi \left[\left\{ (\boldsymbol{\mu}_D - \boldsymbol{\mu}_H)^{\top} (\boldsymbol{\Sigma}_D + \boldsymbol{\Sigma}_H)^{-1} (\boldsymbol{\mu}_D - \boldsymbol{\mu}_H) \right\}^{1/2} \right].$$

Note that when $\boldsymbol{\Sigma}_D = \boldsymbol{\Sigma}_H$, the Fisher discriminating direction is obtained.

Define $\mathcal{A}_\beta(p) = \{\mathbf{x} \in \mathbb{R}^k : \boldsymbol{\beta}^\top \mathbf{x} \geq \boldsymbol{\beta}^\top \boldsymbol{\mu}_H + (\boldsymbol{\beta}^\top \boldsymbol{\Sigma}_H \boldsymbol{\beta})^{1/2} z_p\}$, so that $\mathbb{P}\{\mathbf{x}_H \in \mathcal{A}_\beta(p)\} = p$.

Then, using that $\mathbf{x}_D \sim N(\boldsymbol{\mu}_D, \boldsymbol{\Sigma}_D)$ and denoting as $Z \sim N(0, 1)$, we get that

$$\begin{aligned} \mathbb{P}(\mathbf{x}_D \in \mathcal{A}_\beta(p)) &= \mathbb{P}\left\{\boldsymbol{\beta}^\top \mathbf{x}_D \geq \boldsymbol{\beta}^\top \boldsymbol{\mu}_H + (\boldsymbol{\beta}^\top \boldsymbol{\Sigma}_H \boldsymbol{\beta})^{1/2} z_p\right\} \\ &= \mathbb{P}\left\{Z \geq \frac{\boldsymbol{\beta}^\top (\boldsymbol{\mu}_H - \boldsymbol{\mu}_D) + (\boldsymbol{\beta}^\top \boldsymbol{\Sigma}_H \boldsymbol{\beta})^{1/2} z_p}{(\boldsymbol{\beta}^\top \boldsymbol{\Sigma}_D \boldsymbol{\beta})^{1/2}}\right\} \\ &= 1 - \Phi\left\{\frac{\boldsymbol{\beta}^\top (\boldsymbol{\mu}_H - \boldsymbol{\mu}_D) + (\boldsymbol{\beta}^\top \boldsymbol{\Sigma}_H \boldsymbol{\beta})^{1/2} z_p}{(\boldsymbol{\beta}^\top \boldsymbol{\Sigma}_D \boldsymbol{\beta})^{1/2}}\right\} \\ &= \Phi\left\{\frac{\boldsymbol{\beta}^\top (\boldsymbol{\mu}_D - \boldsymbol{\mu}_H) - (\boldsymbol{\beta}^\top \boldsymbol{\Sigma}_H \boldsymbol{\beta})^{1/2} z_p}{(\boldsymbol{\beta}^\top \boldsymbol{\Sigma}_D \boldsymbol{\beta})^{1/2}}\right\}, \end{aligned} \quad (2)$$

which implies that $\text{ROC}_\beta(p) = \mathbb{P}\{\mathbf{x}_D \in \mathcal{A}_\beta(p)\}$.

From now on, to simplify the discussion below, assume that $\boldsymbol{\Sigma}_j = \boldsymbol{\Sigma}$, for $j = D, H$.

A global ROC curve has been defined as $\text{ROC}(p) = \sup_{\|\boldsymbol{\beta}\|=1} \mathbb{P}\{\mathbf{x}_D \in \mathcal{A}_\beta(p)\}$. Using (2) and that $\boldsymbol{\Sigma}_j = \boldsymbol{\Sigma}$, we obtain that the global ROC curve equals

$$\begin{aligned} \text{ROC}(p) &= \sup_{\|\boldsymbol{\beta}\|=1} \Phi\left\{\frac{\boldsymbol{\beta}^\top (\boldsymbol{\mu}_D - \boldsymbol{\mu}_H) - (\boldsymbol{\beta}^\top \boldsymbol{\Sigma}_H \boldsymbol{\beta})^{1/2} z_p}{(\boldsymbol{\beta}^\top \boldsymbol{\Sigma}_D \boldsymbol{\beta})^{1/2}}\right\} \\ &= \sup_{\|\boldsymbol{\beta}\|=1} \Phi\left\{\frac{\boldsymbol{\beta}^\top (\boldsymbol{\mu}_D - \boldsymbol{\mu}_H)}{(\boldsymbol{\beta}^\top \boldsymbol{\Sigma} \boldsymbol{\beta})^{1/2}} - z_p\right\} = \sup_{\|\boldsymbol{\beta}\|=1} \Phi\left\{\sqrt{2} L(\boldsymbol{\beta}) - z_p\right\}. \end{aligned}$$

Hence, taking into account that $\boldsymbol{\beta}_0$ maximizes $L(\boldsymbol{\beta})$, we obtain that the supremum is a maximum and is attained at $\boldsymbol{\beta}_0 = \boldsymbol{\Sigma}^{-1} (\boldsymbol{\mu}_D - \boldsymbol{\mu}_H)$. Therefore, the global ROC is given by

$$\begin{aligned} \text{ROC}(p) &= \text{ROC}_{\boldsymbol{\beta}_0}(p) = \Phi\left[\left\{\left(\boldsymbol{\mu}_D - \boldsymbol{\mu}_H\right)^\top \boldsymbol{\Sigma}^{-1} (\boldsymbol{\mu}_D - \boldsymbol{\mu}_H)\right\}^{1/2} - z_p\right] \\ &= 1 - \Phi\left[z_p - \left\{\left(\boldsymbol{\mu}_D - \boldsymbol{\mu}_H\right)^\top \boldsymbol{\Sigma}^{-1} (\boldsymbol{\mu}_D - \boldsymbol{\mu}_H)\right\}^{1/2}\right], \end{aligned}$$

meaning that the global ROC curve is the ROC curve associated to the optimal direction with respect to the area under the curve.

Beyond the AUC, the Youden index, which measures the difference between the ROC curve

and the identity function, may also be maximized to obtain the associated optimal direction. In this case, the induced optimality problem searches for the direction $\boldsymbol{\beta}$ such that

$$\text{YI}(\boldsymbol{\beta}) = \max_{c \in \mathbb{R}} \left| \Phi \left\{ \frac{c - \boldsymbol{\beta}^\top \boldsymbol{\mu}_D}{(\boldsymbol{\beta}^\top \boldsymbol{\Sigma} \boldsymbol{\beta})^{1/2}} \right\} - \Phi \left\{ \frac{c - \boldsymbol{\beta}^\top \boldsymbol{\mu}_H}{(\boldsymbol{\beta}^\top \boldsymbol{\Sigma} \boldsymbol{\beta})^{1/2}} \right\} \right| = \max_{c \in \mathbb{R}} \Delta_{\boldsymbol{\beta}}(c)$$

is maximum. Straightforward calculations relegated to the Appendix allow to show that

$$\operatorname{argmax}_{\|\boldsymbol{\beta}\|=1} \text{YI}(\boldsymbol{\beta}) = \frac{\boldsymbol{\Sigma}^{-1}(\boldsymbol{\mu}_D - \boldsymbol{\mu}_H)}{\left\{ (\boldsymbol{\mu}_D - \boldsymbol{\mu}_H)^\top \boldsymbol{\Sigma}^{-1}(\boldsymbol{\mu}_D - \boldsymbol{\mu}_H) \right\}^{1/2}}. \quad (3)$$

Hence, if the covariance matrices are equal, the value $\boldsymbol{\beta}$ maximizing $\text{YI}(\boldsymbol{\beta})$ is proportional to $\boldsymbol{\Sigma}^{-1}(\boldsymbol{\mu}_D - \boldsymbol{\mu}_H)$ and coincides with the direction yielding the maximum AUC.

3 Functional setting

In this section, we consider functional biomarkers belonging to a separable Hilbert space \mathcal{H} which, without loss of generality may be assumed to be $L^2(0,1)$. More precisely, we assume that each functional biomarker $X_j \in \mathcal{H}$, $j = D, H$, and denote as P_j the probability measure related to X_j . From now on, $\|\cdot\|$ and $\langle \cdot, \cdot \rangle$ stand for the norm and the inner product in \mathcal{H} .

Let $\Upsilon : \mathcal{H} \rightarrow \mathbb{R}$ be an operator used as discrimination index to classify a new observation to one of the two classes. Clearly, from this index a related ROC curve may be defined as

$$\text{ROC}_{\Upsilon}(p) = 1 - F_{\Upsilon,D} \left\{ F_{\Upsilon,H}^{-1}(1-p) \right\}, \quad p \in (0,1), \quad (4)$$

where $F_{\Upsilon,D}$ and $F_{\Upsilon,H}^{-1}$ stand for the distribution function and quantile function of $Y_{\Upsilon,j} = \Upsilon(X_j)$, $j = D, H$, respectively, that is, $F_{\Upsilon,j}(u) = P_j \{ \Upsilon(X_j) \leq u \}$. The related area under the curve is then obtained as $\text{AUC}_{\Upsilon} = \mathbb{P}(Y_{\Upsilon,D} > Y_{\Upsilon,H})$. When independent samples $X_{j,i}$, $i = 1, \dots, n_j$, $j = D, H$, are available, estimators of ROC_{Υ} and AUC_{Υ} may be obtained if the discriminating index has a closed form, as it is the case for integral of the biomarker curve, its maximum and/or minimum and other features described in [Jang and Manatunga \(2022\)](#). In this case,

defining, $Y_{j,i} = \Upsilon(X_{j,i})$, $i = 1, \dots, n_j$, $j = D, H$, the ROC estimator is obtained as

$$\widehat{\text{ROC}}(p) = \widehat{\text{ROC}}_{\Upsilon}(p) = 1 - \widehat{F}_{\Upsilon,D} \left\{ \widehat{F}_{\Upsilon,H}^{-1}(1-p) \right\}, \quad p \in (0, 1), \quad (5)$$

where $\widehat{F}_{\Upsilon,D}$ and $\widehat{F}_{\Upsilon,H}^{-1}$ stand for the empirical distribution function and quantile function of the samples $Y_{j,i}$, $i = 1, \dots, n_j$, $j = D, H$, respectively. From the univariate case, the YI estimator can be obtained just by plugging-in the formula $\widehat{\text{YI}} = \widehat{\text{YI}}_{\Upsilon} = \max_{0 < p < 1} \{ \widehat{\text{ROC}}_{\Upsilon}(p) - p \}$, while the AUC estimator is defined as

$$\widehat{\text{AUC}} = \widehat{\text{AUC}}_{\Upsilon} = \frac{1}{n_D n_H} \sum_{i=1}^{n_D} \sum_{\ell=1}^{n_H} \mathbb{I}_{\{Y_{D,i} > Y_{H,\ell}\}}.$$

In the previous situation, the operator chosen to construct the univariate marker is completely known. However, we would like to explore more general situations where Υ may depend on unknown parameters that must be estimated from the data. This may lead to more complex indexes that require, for instance, the estimation of the mean or the covariance operators from both populations. Denote by $\widehat{\Upsilon}$ the predicted discrimination index, and let $\widehat{Y}_{j,i} = \widehat{\Upsilon}(X_{j,i})$, $i = 1, \dots, n_j$, $j = D, H$. Then, the ROC and AUC estimators may be defined as

$$\widehat{\text{ROC}}(p) = \widehat{\text{ROC}}_{\widehat{\Upsilon}}(p) = 1 - \widehat{F}_{\widehat{\Upsilon},D} \left\{ \widehat{F}_{\widehat{\Upsilon},H}^{-1}(1-p) \right\}, \quad p \in (0, 1), \quad (6)$$

$$\widehat{\text{AUC}} = \widehat{\text{AUC}}_{\widehat{\Upsilon}} = \frac{1}{n_D n_H} \sum_{i=1}^{n_D} \sum_{\ell=1}^{n_H} \mathbb{I}_{\{\widehat{Y}_{D,i} > \widehat{Y}_{H,\ell}\}}, \quad (7)$$

where $\widehat{F}_{\widehat{\Upsilon},D}$ and $\widehat{F}_{\widehat{\Upsilon},H}^{-1}$ stand now for the empirical distribution function and quantile function of the predictors $\widehat{Y}_{j,i} = \widehat{\Upsilon}(X_{j,i})$, $i = 1, \dots, n_j$, $j = D, H$, respectively. We proceed similarly with the estimation of the Youden index.

3.1 Linear discriminating index: Maximizing the AUC

In this section, we will work at a population level and define a linear operator $\Upsilon = \Upsilon_{\beta}$ leading to the maximum AUC when both populations have different mean functions. For the sake of

simplicity, as in the multivariate setting, we will consider the situation where X_j are Gaussian processes with mean μ_j and covariance operator Γ_j , denoted $\mathcal{G}(\mu_j, \Gamma_j)$. Then, if $\beta \in \mathcal{H}$, $\|\beta\| = 1$, and we denote $Y_{j,\beta} = \Upsilon_\beta(X_j) = \langle \beta, X_j \rangle$, for $j = D, H$, and by $F_{j,\beta}$ their distribution functions, we have that $Y_{j,\beta} \sim N(\langle \beta, \mu_j \rangle, \langle \beta, \Gamma_j \beta \rangle)$ whenever $\beta \notin \text{Ker}(\Gamma_j)$. It is worth mentioning that if the kernel of Γ_j does not reduce to 0, for any $\beta \in \text{Ker}(\Gamma_j)$, we have that $\mathbb{P}(Y_{j,\beta} = \langle \beta, \mu_j \rangle) = 1$. Let us consider the case where $\mu_j \in \text{Ker}(\Gamma_j)^\perp$, then if $\Gamma_D = \Gamma_H = \Gamma$, $\text{Ker}(\Gamma) \neq \{0\}$ and $\beta \in \text{Ker}(\Gamma)$, we have that $\mathbb{P}(Y_{j,\beta} = 0) = 1$, for $j = D, H$, so the two populations cannot be distinguished in such directions.

As in the multivariate case for each fixed $\beta \in \mathcal{H}$, $\|\beta\| = 1$, $\beta \notin \text{Ker}(\Gamma_D) \cap \text{Ker}(\Gamma_H)$, the AUC associated to the new independent biomarkers $Y_{j,\beta}$ is given by

$$\text{AUC}(\beta) = \mathbb{P}(Y_{D,\beta} > Y_{H,\beta}) = \Phi \left[\frac{\langle \beta, \mu_D - \mu_H \rangle}{\{\langle \beta, (\Gamma_H + \Gamma_D) \beta \rangle\}^{1/2}} \right].$$

As in the finite-dimensional case, if $\mu_H = \mu_D$ and $\Gamma_H = \Gamma_D$, the projected univariate biomarkers $Y_{j,\beta}$ cannot be distinguished. Furthermore, if $\mu_D = \mu_H$ but $\Gamma_H \neq \Gamma_D$ using a linear rule will not be a suitable choice in practice since $\text{AUC}(\beta) = 1/2$, for any $\beta \in \mathcal{H}$, so the problem of searching for a direction maximizing the AUC is not adequate and other rules should be employed. For that reason, along this section we will assume $\mu_D \neq \mu_H$.

Then, if we denote $\Gamma_A = (\Gamma_H + \Gamma_D)/2$, the element β_0 maximizing $\text{AUC}(\beta)$ may be obtained up to a positive constant as $\beta_0 = \text{argmax}_{\beta \neq 0} L(\beta)$, where

$$L(\beta) = \frac{\langle \beta, \mu_D - \mu_H \rangle}{(2\langle \beta, \Gamma_A \beta \rangle)^{1/2}}. \quad (8)$$

It is worth mentioning the analogy with the expression given in (1). In practice, the population parameters in equation (8) need to be estimated as will be described in the next Section.

Unlike the multivariate case and as in canonical correlation, this maximization problem poses some challenges due to its infinite-dimensional structure. The major problem is due to the fact that the operator $\Gamma_A = (\Gamma_H + \Gamma_D)/2$ is compact and then it does not have an inverse. To clarify the difficulties and the relation to canonical correlation, let X be such that

$X \mid G = 1 \sim X_D$ and $X \mid G = 0 \sim X_H$ with G a binary variable indicating the group membership, such that $\mathbb{P}(G = 1) = \pi_D$ and denote $\pi_H = 1 - \pi_D$.

Lemma 3.1. *Let $L_{\text{POOL}}(\beta)$ be defined as*

$$L_{\text{POOL}}(\beta) = \frac{\langle \beta, \mu_D - \mu_H \rangle}{(2\langle \beta, \Gamma_{\text{POOL}}\beta \rangle)^{1/2}}, \quad (9)$$

where $\Gamma_{\text{POOL}} = \pi_D\Gamma_D + \pi_H\Gamma_H$. Then, if $\mu_D \neq \mu_H$

- a) for any $\beta \notin \text{Ker}(\Gamma_D) \cap \text{Ker}(\Gamma_H)$, $\text{corr}^2(\langle \beta, X \rangle, G) = \pi_D\pi_H [1 - \{1 + L_{\text{POOL}}^2(\beta)\}^{-1}]$.
- b) When $\pi_D = 1/2$ or when $\Gamma_H = \Gamma_D$, the problem of maximizing the AUC and that of maximizing $\text{corr}(\langle \beta, X \rangle, G)$ coincide.

In the sequel Γ will denote either Γ_{POOL} or Γ_A . Note that when $\Gamma_H = \Gamma_D$, then $\Gamma_{\text{POOL}} = \Gamma_A = \Gamma$. The following proposition provides an explicit expression for the direction maximizing $L_{\text{POOL}}^2(\beta)$ and/or the AUC.

From now on denote $\lambda_1 \geq \lambda_2 \geq \dots$ the eigenvalues of Γ and ϕ_j the corresponding eigenfunctions.

Proposition 3.2. *Let us assume that the eigenvalues λ_j of Γ are all positive and define the linear space $\mathcal{R}(\Gamma) = \{y \in \mathcal{H} : \sum_{\ell \geq 1} \lambda_\ell^{-2} \langle y, \phi_\ell \rangle^2 < \infty\}$, and the inverse of $\Gamma : \mathcal{R}(\Gamma) \rightarrow \mathcal{H}$ as $\Gamma^{-1}(y) = \sum_{\ell \geq 1} \lambda_\ell^{-1} \langle y, \phi_\ell \rangle \phi_\ell$, for any $y \in \mathcal{R}(\Gamma)$. Furthermore, assume that $\mu_D - \mu_H \in \mathcal{R}(\Gamma)$ and $\mu_D \neq \mu_H$. Then, if $\Gamma = \Gamma_{\text{POOL}}$ and β_0 stands for the value maximizing $L_{\text{POOL}}^2(\beta)$ or if $\Gamma = \Gamma_A$ and β_0 stands for the value maximizing the AUC, then $\beta_0 = (\pi_D\pi_H)^{1/2} \Gamma^{-1}(\mu_D - \mu_H)$.*

Remark 3.1. *It is worth mentioning that similar arguments enable to extend the results of Proposition 3.2 to settings more general than the Gaussian. In fact, straightforward arguments allow to show that β_0 still maximizes the AUC if the biomarkers have an elliptical distribution with scatter operators, as defined in Bali and Boente (2009) and studied in Boente et al. (2014). In what follows we briefly present the arguments leading to this conclusion.*

To state the definition of elliptical distributions in a functional setting, we will first remind the basic concept of elliptical distributions in \mathbb{R}^k . Recall that a random vector $\mathbf{z} \in \mathbb{R}^k$ is said

to have a k -dimensional spherical distribution if its distribution is invariant under orthogonal transformations. In general, the characteristic function of a spherically distributed $\mathbf{x} \in \mathbb{R}^k$ is of the form $\psi_{\mathbf{x}}(\mathbf{t}_k) = \varphi(\mathbf{t}_k^\top \mathbf{t}_k)$ for $\mathbf{t}_k \in \mathbb{R}^k$, and any distribution in \mathbb{R}^k having a characteristic function of this form is a spherical distribution. Hence, we can denote a spherically distributed vector as $\mathbf{x} \sim \mathcal{S}_k(\varphi)$, which is convenient since, for $\mathbf{x}^\top = (\mathbf{x}_1^\top, \mathbf{x}_2^\top)$ with $\mathbf{x}_1 \in \mathbb{R}^m$, we have that $\mathbf{x}_1 \sim \mathcal{S}_m(\varphi)$.

Elliptical distributions in \mathbb{R}^k correspond to distributions obtained from affine transformations of spherically distributed random vectors in \mathbb{R}^k . More precisely, for a given matrix $\mathbf{A} \in \mathbb{R}^{k \times k}$ and a vector $\boldsymbol{\mu} \in \mathbb{R}^k$, the distribution of $\mathbf{x} = \mathbf{A}\mathbf{z} + \boldsymbol{\mu}$ when $\mathbf{z} \sim \mathcal{S}_k(\varphi)$ is said to have an elliptical distribution, denoted $\mathbf{x} \sim \mathcal{E}_k(\boldsymbol{\mu}, \boldsymbol{\Sigma}, \varphi)$, where $\boldsymbol{\Sigma} = \mathbf{A}\mathbf{A}^\top$. When first moment exists, $\mathbb{E}(\mathbf{X}) = \boldsymbol{\mu}$. Furthermore, when second moments exist then the covariance matrix of \mathbf{x} is proportional to $\boldsymbol{\Sigma}$.

It is easy to see that the characteristic function of \mathbf{x} equals $\psi_{\mathbf{x}}(\mathbf{t}) = \exp(i\mathbf{t}^\top \boldsymbol{\mu})\varphi(\mathbf{t}^\top \boldsymbol{\Sigma}\mathbf{t})$. Hence, the scatter matrix $\boldsymbol{\Sigma}$ is confounded with the function φ in the sense that, for any $c > 0$, $\mathcal{E}_k(\boldsymbol{\mu}, \boldsymbol{\Sigma}, \varphi) \sim \mathcal{E}_k(\boldsymbol{\mu}, c\boldsymbol{\Sigma}, \varphi_c)$ where $\varphi_c(w) = \varphi(w/c)$. For that reason, henceforth, we will assume that the characteristic function φ is chosen so that the covariance matrix of \mathbf{x} equals $\boldsymbol{\Sigma}$.

An important property of elliptical distributions, is that the sum of independent elliptical random vectors with the same scatter matrix $\boldsymbol{\Sigma}$ is elliptical, see [Hult and Lindskog \(2002\)](#) and [Frahm \(2004\)](#). This fact is important in what follows, since it implies that if $\mathbf{x}_D \sim \mathcal{E}_k(\boldsymbol{\mu}_D, \boldsymbol{\Sigma}, \varphi_D)$ and $\mathbf{x}_H \sim \mathcal{E}_k(\boldsymbol{\mu}_H, \boldsymbol{\Sigma}, \varphi_H)$ are independent, then $\mathbf{x}_D - \mathbf{x}_H \sim \mathcal{E}_k(\boldsymbol{\mu}_D - \boldsymbol{\mu}_H, \boldsymbol{\Sigma}, \varphi_D \times \varphi_H)$ and $\boldsymbol{\beta}^\top(\mathbf{x}_D - \mathbf{x}_H) \sim \boldsymbol{\beta}^\top(\boldsymbol{\mu}_D - \boldsymbol{\mu}_H) + z(\boldsymbol{\beta}^\top \boldsymbol{\Sigma} \boldsymbol{\beta})^{1/2}$, where the random variable z has a symmetric distribution G_0 with characteristic function $\varphi_z(t) = \varphi_D(t^2) \varphi_H(t^2)$.

[Bali and Boente \(2009\)](#) define elliptical distributed random elements in a separable Hilbert-space \mathcal{H} as follows. The random element X is said to have an elliptical distribution $\mathcal{E}(\boldsymbol{\mu}, \Gamma, \varphi)$ with parameters $\boldsymbol{\mu} \in \mathcal{H}$ and $\Gamma : \mathcal{H} \rightarrow \mathcal{H}$ a self-adjoint, positive semi-definite and compact operator if and only if for any linear and bounded operator $A : \mathcal{H} \rightarrow \mathbb{R}^k$, we have that $AX \sim \mathcal{E}_k(A\boldsymbol{\mu}, A\Gamma A^*, \varphi)$ where $A^* : \mathbb{R}^k \rightarrow \mathcal{H}$ stands for the adjoint operator of A . As noted in [Boente et al. \(2014\)](#), $X \sim \mathcal{E}(\boldsymbol{\mu}, \Gamma, \varphi)$ if and only if $\langle a, X \rangle \sim \mathcal{E}_1(\langle a, \boldsymbol{\mu} \rangle, \langle a, \Gamma a \rangle, \varphi)$ for all $a \in \mathcal{H}$.

The above discussion implies that, if $X_j \sim \mathcal{E}(\mu_j, \Gamma, \varphi_j)$, for $j = D, H$, then the projected biomarkers AUC can be expressed as $AUC(\beta) = \mathbb{P}(Y_{D,\beta} > Y_{H,\beta}) = G_0 \left\{ \langle \beta, \mu_D - \mu_H \rangle / (\langle \beta, \Gamma \beta \rangle)^{1/2} \right\}$, with G_0 a distribution function symmetric around 0, that is, $G_0(t) = 1 - G_0(-t)$. Therefore, the value maximizing the AUC is still the one maximizing $L_{\text{POOL}}(\beta)$ in (9) and is given in Proposition 3.2.

3.2 Estimating the linear projection index

As mentioned above, general discriminating indexes require the estimation of unknown parameters. In this section, we focus on the linear index $\Upsilon(X) = \langle \beta_0, X \rangle$, where β_0 maximizes the AUC as given in Proposition 3.2.

Suppose that independent samples $X_{j,i}$, $i = 1, \dots, n_j$, $j = D, H$, are available. As shown by Leurgans et al. (1993) for the case of canonical correlation between two functional random elements, the sample maximum correlation can attain the value 1, for proper directions. The same arises in the present situation, where the sample version of the AUC may lead to values close to 1 for proper directions, meaning that the maximizer of $\widehat{L}(\beta)$ or equivalently of $\widehat{AUC}(\beta)$ will not provide relevant information.

As in functional canonical correlation, the problem may be overcome using increasing finite-dimensional linear spaces and/or penalizations. More precisely, let $D\alpha = \alpha''$ and $\Psi(\alpha) = \|D\alpha\|$, then we can penalize the denominator in $L(\beta)$ to define

$$\widehat{L}_\lambda(\beta) = \frac{\langle \beta, \widehat{\mu}_D - \widehat{\mu}_H \rangle}{\left\{ \langle \beta, \widehat{\Gamma} \beta \rangle + \lambda \Psi(\beta) \right\}^{1/2}},$$

where $\widehat{\mu}_D$, $\widehat{\mu}_H$ are estimators of μ_D and μ_H and $\widehat{\Gamma}$ is an estimator of Γ_A , such as their sample versions. A typical choice for $\widehat{\mu}_j$ is the sample mean $\overline{X}_j = (1/n_j) \sum_{i=1}^{n_j} X_{j,i}$. When both samples have the same covariance matrix a possible estimator for $\Gamma_A = \Gamma_{\text{POOL}}$ is the pooled covariance operator given by $\widehat{\Gamma}_{\text{POOL}} = (n_D/n) \widehat{\Gamma}_D + (n_H/n) \widehat{\Gamma}_H$, with $n = n_D + n_H$ and $\widehat{\Gamma}_j = (1/n_j) \sum_{i=1}^{n_j} (X_{j,i} - \overline{X}_j) \otimes (X_{j,i} - \overline{X}_j)$, while if the practitioner suspects that $\Gamma_D \neq \Gamma_H$, it is

better to choose $\widehat{\Gamma} = \widehat{\Gamma}_A$, where $\widehat{\Gamma}_A = (\widehat{\Gamma}_D + \widehat{\Gamma}_H)/2$. We seek for the values $\widehat{\beta}$ maximizing $\widehat{L}_\lambda(\beta)$ over the set $\{\beta \in \mathcal{H}_k : \|\beta\| = 1\}$ with \mathcal{H}_k a finite-dimensional linear space of dimension k , such as the one spanned by the first elements of the Fourier basis. An adaptive basis, as the one spanned by the first eigenfunctions of the pooled sample operator may also be chosen. Note that if no dimension reduction is performed, that is, when $\widehat{\beta}$ maximizes $\widehat{L}_\lambda(\beta)$ over the unit ball in \mathcal{H} , the procedure corresponds to the optimal scoring approach to discriminant analysis described in [Ramsay and Silverman \(2005\)](#).

As mentioned above, once the direction $\widehat{\beta}$ is obtained, the estimated linear discrimination index, denoted $\widehat{\Upsilon}_{\text{LIN}}$, equals $\widehat{\Upsilon}(X) = \widehat{\Upsilon}_{\text{LIN}}(X) = \Upsilon_{\widehat{\beta}}(X) = \langle \widehat{\beta}, X \rangle$ may be constructed, leading to the real-valued predictors $\widehat{Y}_{j,i} = \widehat{\Upsilon}(X_{j,i}) = \Upsilon_{\widehat{\beta}}(X_{j,i}) = \langle \widehat{\beta}, X_{j,i} \rangle$, $i = 1, \dots, n_j$, $j = D, H$ from which the ROC curve estimator may be constructed as

$$\widehat{\text{ROC}}(p) = \widehat{\text{ROC}}_{\Upsilon_{\widehat{\beta}}}(p) = 1 - \widehat{F}_D \left\{ \widehat{F}_H^{-1}(1-p) \right\}, \quad p \in (0, 1), \quad (10)$$

where $\widehat{F}_D = \widehat{F}_{\Upsilon_{\widehat{\beta}, D}}$ and $\widehat{F}_H^{-1} = \widehat{F}_{\Upsilon_{\widehat{\beta}, H}}^{-1}$ stand for the empirical distribution function and quantile function of the predictors $\widehat{Y}_{j,i}$, $i = 1, \dots, n_j$, $j = D, H$, respectively.

3.3 Definition of a quadratic discrimination index

In the situations where the covariance operators differ between populations, some improvements to the linear index defined above may be obtained in terms of the AUC by considering alternative indexes. As mentioned above, the situation is even worst when population means are equal in which case, the linear rule is an improper one. For instance, as it is well known, for multivariate normally distributed biomarkers the quadratic discriminating rule offers a procedure with better classification rates than the linear one when the covariance matrices of both populations are different from each other, in particular for unbalanced samples. We will explore a generalization of these ideas in the functional framework.

Measuring differences between covariance operators or even between covariance matrices is difficult, we refer to [Flury \(1988\)](#) who mentioned that “*In contrast to the univariate situation,*

inequality is not just inequality—there are indeed many ways in which covariance matrices can differ”. For that reason, in the functional literature some parsimonious models have been considered, including models with proportional covariance operators or models assuming that both covariance operators share the same eigenfunctions. In this section, we focus on these settings and we will use the basis of principal directions to reduce the dimension, even when any basis can be chosen to project the data and construct the quadratic index when we suspect that differences between covariance operators arise.

A natural extension of functional principal components to several populations, which corresponds to the generalization of the common principal components model introduced by [Flury \(1984\)](#) to the functional setting, is to assume that the covariance operators Γ_j have common eigenfunctions ϕ_ℓ but possible different eigenvalues $\lambda_{j,\ell}$, i.e.,

$$\Gamma_j = \sum_{\ell=1}^{\infty} \lambda_{j,\ell} \phi_\ell \otimes \phi_\ell, \quad (11)$$

where, to identify the directions, we assume that the eigenvalues of the healthy population are ordered in decreasing order, that is, $\lambda_{H,1} \geq \lambda_{H,2} \geq \dots \geq \lambda_{H,\ell} \geq \lambda_{H,\ell+1} \geq \dots$. This model is usually denoted the functional common principal component model (FCPC) and provides a framework for analysing different population data that share their main modes of variation ϕ_1, ϕ_2, \dots using a parsimonious approach. When the eigenvalues preserve the order across populations, i.e., if

$$\lambda_{j,1} \geq \lambda_{j,2} \geq \dots \geq \lambda_{j,\ell} \geq \lambda_{j,\ell+1} \geq \dots, \text{ for } j = D, H, \quad (12)$$

as assumed, for instance, in [Benko and Härdle \(2005\)](#) and [Boente et al. \(2010\)](#), the common directions will represent, as in the one–population setting, the main modes of variation for each population. Furthermore, in such a situation, the operators Γ_{POOL} and Γ_A will also have the same principal directions and in the same order.

However, if the largest k eigenvalues do not preserve the order among populations, that is, if we only have $\lambda_{j,\ell} \geq \lambda_{j,k+1} \geq \lambda_{j,k+2} \geq \dots \geq 0$, for $j = D, H$ and $\ell = 1, \dots, k$, the eigenfunctions

ϕ_1, \dots, ϕ_k represent the modes of variation that are common to each group, even when the ordering across groups changes. As mentioned in Coffey et al. (2011), the eigenvalues $\lambda_{j,\ell}$, $\ell = 1, \dots, k$, determine the order of the common directions in each group and may allow to study the differences in the distribution of the variation across groups. The functional common principal component model may be used to reduce the dimensionality of the data, retaining the maximum variability present in each of the populations.

Assume that the covariance operators of both populations satisfy a FCPC model and that (12) holds, then the first k principal directions provide a natural linear space where the data projection may be performed. More precisely, define the k -dimensional vectors $\mathbf{x}_j = (\langle \phi_1, X_j \rangle, \dots, \langle \phi_k, X_j \rangle)^\top$, $j = D, H$, where ϕ_ℓ , $\ell = 1, \dots, k$, stand for the first k common principal directions. Usually in practice the dimension k is chosen so as to explain a given percentage of the total variability measured through the eigenvalues of an estimator of Γ_{POOL} .

Note that when X_j , $j = D, H$, are Gaussian processes with mean μ_j and covariance operators Γ_j satisfying (11), then $\mathbf{x}_{j,i} \sim N(\boldsymbol{\mu}_j, \boldsymbol{\Sigma}_j)$ with $\boldsymbol{\mu}_j = (\mu_{j,1}, \dots, \mu_{j,k})^\top$, $\mu_{j,\ell} = \langle \phi_\ell, \mu_j \rangle$ and $\boldsymbol{\Sigma}_j = \text{DIAG}(\lambda_{j,1}, \dots, \lambda_{j,k})$, meaning that $\mathbf{x}_{j,1}$, $j = D, H$, fulfil the common principal components model (CPC) considered in Flury (1984). From these projections, if $\lambda_{j,k} > 0$, for $j = D, H$, a quadratic discriminant index may be defined as

$$\Upsilon_{\text{QUAD}}(X) = \Upsilon_{\boldsymbol{\Lambda}_0, \boldsymbol{\alpha}_0}(X) = -\mathbf{x}^\top \boldsymbol{\Lambda}_0 \mathbf{x} + 2\boldsymbol{\alpha}_0^\top \mathbf{x},$$

where $\mathbf{x} = (\langle \phi_1, X \rangle, \dots, \langle \phi_k, X \rangle)^\top$, $\boldsymbol{\Lambda}_0 = \boldsymbol{\Sigma}_D^{-1} - \boldsymbol{\Sigma}_H^{-1}$ and $\boldsymbol{\alpha}_0 = \boldsymbol{\Sigma}_D^{-1} \boldsymbol{\mu}_D - \boldsymbol{\Sigma}_H^{-1} \boldsymbol{\mu}_H$. Note that under the FCPC model

$$\begin{aligned} \boldsymbol{\Lambda}_0 &= \text{DIAG} \left(\frac{\lambda_{H,1} - \lambda_{D,1}}{\lambda_{D,1} \lambda_{H,1}}, \dots, \frac{\lambda_{H,k} - \lambda_{D,k}}{\lambda_{D,k} \lambda_{H,k}} \right) = \text{DIAG}(\Lambda_1, \dots, \Lambda_k) \\ \boldsymbol{\alpha}_0 &= \begin{pmatrix} \frac{\mu_{D,1} \lambda_{H,1} - \mu_{H,1} \lambda_{D,1}}{\lambda_{D,1} \lambda_{H,1}} \\ \vdots \\ \frac{\mu_{D,k} \lambda_{H,k} - \mu_{H,k} \lambda_{D,k}}{\lambda_{D,k} \lambda_{H,k}} \end{pmatrix} = \begin{pmatrix} \frac{\mu_{D,1}}{\lambda_{D,1}} - \frac{\mu_{H,1}}{\lambda_{H,1}} \\ \vdots \\ \frac{\mu_{D,k}}{\lambda_{D,k}} - \frac{\mu_{H,k}}{\lambda_{H,k}} \end{pmatrix}. \end{aligned}$$

Besides, to be precise we should write $\Upsilon_{\text{QUAD}}(X) = \Upsilon_{k,\text{QUAD}}(X)$ since it depends on the number of selected common directions. However, we have decided to omit its dependence on k to simplify the notation.

Under mild assumptions, Proposition 3.3 below provides an expression of the quadratic discriminating rule which suggests an asymptotic expression for it, as the number of principal directions increases.

Proposition 3.3. *Assume that Γ_j satisfy (11) and (12), with $\lambda_{j,\ell} > 0$, for $j = D, H$ and $\ell \geq 1$, and that $\mu_j \in \mathcal{R}(\Gamma_j)$. Denote $\alpha_0 = \Gamma_D^{-1}\mu_D - \Gamma_H^{-1}\mu_H$ and let $A : \mathcal{H} \rightarrow \mathbb{R}^k$ stand for the projection operator $Ay = (\langle \phi_1, y \rangle, \dots, \langle \phi_k, y \rangle)^\top$, for any $y \in \mathcal{H}$. Then,*

a) $\alpha_0^\top \mathbf{x} = \langle A^* A \alpha_0, X \rangle = \sum_{\ell=1}^k \langle \alpha_0, \phi_\ell \rangle \langle \phi_\ell, X \rangle$ where $A^* : \mathbb{R}^k \rightarrow \mathcal{H}$ stands for the adjoint operator of A given by $A^* \mathbf{u} = \sum_{\ell=1}^k u_\ell \phi_\ell$.

b) $\mathbf{x}^\top \Lambda_0 \mathbf{x} = \|A\Gamma_D^{-1/2} X\|^2 - \|A\Gamma_H^{-1/2} X\|^2$, if $X \in \mathcal{R}(\Gamma_D^{1/2}) \cap \mathcal{R}(\Gamma_H^{1/2})$. Hence,

$$\Upsilon_{\text{QUAD}}(X) = - \left(\|A\Gamma_D^{-1/2} X\|^2 - \|A\Gamma_H^{-1/2} X\|^2 \right) + 2 \langle A^* A \alpha_0, X \rangle.$$

Then, for any $X \in \mathcal{R}(\Gamma_D^{1/2}) \cap \mathcal{R}(\Gamma_H^{1/2})$, if the number k of principal directions increases to infinity the index $\Upsilon_{\text{QUAD}}(X)$ converges to $\Upsilon(X) = - \left(\|\Gamma_D^{-1/2} X\|^2 - \|\Gamma_H^{-1/2} X\|^2 \right) + 2 \langle \alpha_0, X \rangle$.

Two facts should be highlighted regarding Proposition 3.3. On the one hand, note that from the Karhunen–Loève expansion of the Gaussian processes X_j , we get that $\mathbb{P}\{X_j - \mu_j \in \mathcal{R}(\Gamma_j^{1/2})\} = 0$. Effectively, the mentioned expansion leads to $X_j - \mu_j = \sum_{\ell \geq 1} \xi_{j,\ell} \phi_\ell$ where $\xi_{j,\ell}$ are independent and $\xi_{j,\ell} \sim N(0, \lambda_{j,\ell})$ which implies that $\langle X_j, \phi_\ell \rangle^2 / \lambda_{j,\ell} = \xi_{j,\ell}^2 / \lambda_{j,\ell} \sim \chi_1^2$, meaning that $X_j - \mu_j \notin \mathcal{R}(\Gamma_j^{1/2})$ with probability 1. Thus, the linear space where Υ is defined is too small to define a proper discriminating rule. In this sense, $\Upsilon_{\text{QUAD}} = \Upsilon_{k,\text{QUAD}}$ circumvents the *curse of dimensionality* imposed by the infinite–dimensional structure of the model and provides a finite–dimensional approximation of Υ whose range is the whole space \mathcal{H} ensuring the definition of a proper rule. On the other hand, the requirement that $\lambda_{j,\ell} > 0$, for $j = D, H$ and $\ell \geq 1$, is

needed to guarantee that Γ_j has an inverse over $\mathcal{R}(\Gamma_j)$. Moreover, if $\lambda_{j,\ell} = 0$, for $\ell \geq k_0$, then the quadratic rule $\Upsilon_{k,\text{QUAD}}$ may only be defined when $k < k_0$, since otherwise the matrix Σ_j will be singular.

Clearly, the principal directions are unknown and must be estimated from the sample. These estimators denoted $\hat{\phi}_\ell$, $\ell = 1, \dots, k$, may be obtained, for instance, as the eigenfunctions related to the largest k eigenvalues of the sample pooled covariance operator, see for instance, [Boente et al. \(2010\)](#). We then may define the k -dimensional vectors $\hat{\mathbf{x}}_{j,i} = (\langle \hat{\phi}_1, X_{j,i} \rangle, \dots, \langle \hat{\phi}_k, X_{j,i} \rangle)^\top$, $i = 1, \dots, n_j$, $j = D, H$, which provide predictors of the finite-dimensional vectors $\mathbf{x}_{j,i} = (\langle \phi_1, X_{j,i} \rangle, \dots, \langle \phi_k, X_{j,i} \rangle)^\top$.

In this case, the quadratic discrimination rule provides a better approach to classify a new observation to each group. For that reason, we propose to consider as estimated quadratic index

$$\hat{\Upsilon}_{\text{QUAD}}(X) = \Upsilon_{\hat{\Lambda}, \hat{\alpha}}(X) = -\mathbf{x}^\top \hat{\Lambda} \mathbf{x} + 2\hat{\alpha}^\top \mathbf{x}, \quad (13)$$

where $\mathbf{x} = (\langle \hat{\phi}_1, X \rangle, \dots, \langle \hat{\phi}_k, X \rangle)^\top$, $\hat{\Lambda} = \hat{\Sigma}_D^{-1} - \hat{\Sigma}_H^{-1}$, $\hat{\alpha} = \hat{\Sigma}_D^{-1} \hat{\boldsymbol{\mu}}_D - \hat{\Sigma}_H^{-1} \hat{\boldsymbol{\mu}}_H$ where $\hat{\boldsymbol{\mu}}_j$ and $\hat{\Sigma}_j$ stand for the sample mean and covariance matrix of $\{\mathbf{x}_{j,i}\}_{i=1}^{n_j}$, $j = D, H$, respectively.

Again, the estimated ROC curve may be defined as

$$\widehat{\text{ROC}}(p) = \widehat{\text{ROC}}_{\hat{\Upsilon}_{\text{QUAD}}}(p) = 1 - \hat{F}_D \left\{ \hat{F}_H^{-1}(1-p) \right\}, \quad p \in (0, 1), \quad (14)$$

where $\hat{F}_D = \hat{F}_{\hat{\Upsilon}_{\text{QUAD},D}}$ and $\hat{F}_H^{-1} = \hat{F}_{\hat{\Upsilon}_{\text{QUAD},H}}^{-1}$ denote the empirical distribution function and quantile function of the predictors $\hat{Y}_{j,i} = \hat{\Upsilon}_{\text{QUAD}}(X_{j,i})$, $i = 1, \dots, n_j$, $j = D, H$, respectively.

As mentioned in [Flury and Schmid \(1992\)](#), for the multivariate setting, the quadratic rule may be adapted to the setting of CPC or proportional models estimating the parameters under these constraints. This procedure may lead to more stable estimations than those obtained using the sample covariance estimators $\hat{\Sigma}_j$, specially for small samples, leading to better rates of misclassification and probably to higher AUC values, when the most parsimonious among all the correct models is used for discrimination. We leave the interesting topic of comparing the performance of the ROC curve estimators obtained using constrained estimators for future

research.

4 Consistency results

In this section, we establish consistency results for some discriminating indexes under mild assumptions. In particular, our results include cases where the discriminating index depends on a known operator, as those considered in [Jang and Manatunga \(2022\)](#). We also analyse the situation where the index $\Upsilon(X)$ is linear and defined by means of a coefficient β_0 that may be known as in the case of $\Upsilon(X) = \int_{\mathcal{I}} X(t)dt$ where $\beta_0 \equiv 1$ or unknown as it arises when considering, for instance, $\Upsilon(X) = \langle \mu_D - \mu_H, X \rangle$ where $\beta_0 = \mu_D - \mu_H$ or $\Upsilon(X) = \langle \beta_0, X \rangle$, where β_0 maximizes $L_{\text{POOL}}(\beta)$. Besides, we study the situation of the quadratic discrimination rule defined in [Section 3.3](#), when the number of principal directions is fixed.

Let $X_j \sim P_j$, $j = D, H$, be a multivariate or functional biomarker. Consider $\Upsilon : \mathcal{H} \rightarrow \mathbb{R}$ a discrimination index used to define the ROC curve ROC_{Υ} as in [\(4\)](#), where for simplicity we denote $F_j = F_{\Upsilon,j}$ the distribution function of $Y_j = \Upsilon(X_j)$, $j = D, H$. Recall that the related area under the curve equals $\text{AUC}_{\Upsilon} = \mathbb{P}(Y_{\Upsilon,D} > Y_{\Upsilon,H})$.

The estimator of the ROC curve is obtained in many situations by means of an estimated discrimination index $\widehat{\Upsilon}$, unless Υ is completely known in which case in what follows $\widehat{\Upsilon} = \Upsilon$. This estimator is based on independent samples $X_{j,i}$, $i = 1, \dots, n_j$, $j = D, H$, which allow to define $\widehat{\text{ROC}} = \widehat{\text{ROC}}_{\widehat{\Upsilon}}$ and $\widehat{\text{AUC}} = \widehat{\text{AUC}}_{\widehat{\Upsilon}}$ as in [\(6\)](#) and [\(7\)](#), respectively. For simplicity, we label $\widehat{F}_j = \widehat{F}_{\widehat{\Upsilon},j}$ for the empirical distribution function of the predictors $\widehat{Y}_{j,i} = \widehat{\Upsilon}(X_{j,i})$, $i = 1, \dots, n_j$, $j = D, H$. It is worth noting that the asymptotic results we derive are based on the assumption that sample sizes grow to infinity, that is $n_j \rightarrow \infty$, $j = D, H$.

In order to derive consistency results for the ROC curve estimators $\widehat{\text{ROC}}_{\widehat{\Upsilon}}$, we will need the following assumptions.

A1 $F_H = F_{H,\Upsilon} : \mathbb{R} \rightarrow (0, 1)$ has density $f_{H,\Upsilon}$ such that $f_{H,\Upsilon}(u) > 0$, for all $u \in \mathbb{R}$.

A2 $F_D = F_{D,\Upsilon} : \mathbb{R} \rightarrow (0, 1)$ is continuous.

A3 $\|\widehat{F}_j - F_j\|_\infty \xrightarrow{a.s.} 0$, $j = D, H$.

Assumptions **A1** and **A2** are the usual assumptions required to obtain consistency when using a univariate biomarker. Some situations where **A3** holds are discussed in Remark 4.1 and below.

Theorem 4.1 below states the consistency for the studied estimators of the ROC curve.

Theorem 4.1. *Let $\{X_{j,i}\}_{i=1}^{n_j}$, $j = D, H$, be independent observations and let $\widehat{\Upsilon}$ be an estimator of Υ . Assume that Assumptions **A1–A3** hold. Then,*

$$a) \sup_{0 < p < 1} |\widehat{ROC}(p) - ROC(p)| \xrightarrow{a.s.} 0,$$

$$b) \widehat{AUC} \xrightarrow{a.s.} AUC,$$

$$c) \widehat{YI} \xrightarrow{a.s.} YI.$$

Remark 4.1. *Note that the Glivenko–Cantelli Theorem entails that Assumption **A3** holds when Υ is known. Hence, when the discriminating index is linear $\Upsilon(X) = \langle \beta_0, X \rangle$ where β_0 is known, Theorem 4.1 provides mild conditions ensuring consistency of the estimated ROC curve.*

More precisely, if the distribution function $F_{j,\Upsilon}$ of $Y_j = \Upsilon(X_j)$ are continuous, for $j = D, H$, and $F_{H,\Upsilon}$ has density $f_{H,\Upsilon}$ such that $f_{H,\Upsilon}(u) > 0$, for all $u \in \mathbb{R}$, then the conclusion of Theorem 4.1 holds for the estimator given in (5).

Theorem 4.1 also provides consistency results for the discriminating indexes defined in Jang and Manatunga (2022), $\Upsilon(X) = \int_{\mathcal{I}} X(t)dt$, $\Upsilon(X) = \int_{\mathcal{I}} X'(t)dt = X(b) - X(a)$, $\Upsilon(X) = \int_{\mathcal{I}} X''(t)dt = X'(b) - X'(a)$ as well as $\Upsilon(X) = \max_{t \in \mathcal{I}} X(t)$ and $\Upsilon(X) = \min_{t \in \mathcal{I}} X(t)$.

By means of Theorem 4.1, Theorems 4.2 and 4.3 below state consistency results when the discriminating index is linear. More precisely, let β_0 be the direction in which we project in order to determine the ROC curve, i.e., we assume that $\Upsilon(X) = \langle \beta_0, X \rangle$. Furthermore, denote $\Upsilon_\beta(X) = \langle X, \beta \rangle$ and $F_{\beta,j} = F_{\Upsilon_\beta,j}$ the distribution of $\Upsilon_\beta(X_j)$ when $X_j \sim P_j$, while for simplicity, as above, we will call F_j that corresponding to $F_{\beta_0,j}$.

From now on, $\widehat{\beta}$ stands for an estimator of β_0 which we will assume to be consistent. We denote $\widehat{F}_{\beta,j} = \widehat{F}_{\Upsilon_{\beta,j}}$ the empirical distribution related of $\Upsilon_{\beta}(X_{j,i}) = \langle X_{j,i}, \beta \rangle$, $i = 1, \dots, n_j$, $j = D, H$, while, to abbreviate, \widehat{F}_j stands for $\widehat{F}_{\widehat{\beta},j}$. The ROC curve associated to $\Upsilon(X) = \Upsilon_{\beta_0}(X) = \langle \beta_0, X \rangle$ can be written as $\text{ROC}(p) = 1 - F_D\{F_H^{-1}(1-p)\}$, while its estimator equals $\widehat{\text{ROC}}(p) = 1 - \widehat{F}_D\{\widehat{F}_H^{-1}(1-p)\}$. Without loss of generality, we may assume that $\|\beta_0\| = 1$ and $\|\widehat{\beta}\| = 1$.

Assumptions **A1** and **A2** state that $F_{\beta_0,j}$ are continuous for $j = D, H$ and $F_{\beta_0,H}$ has a strictly positive density $f_{\beta_0,H}$. The key point is to provide conditions ensuring that Assumption **A3** holds.

In the finite-dimensional setting, Theorem 4.2 ensures that Assumption **A3** is a consequence of the strong consistency of $\widehat{\beta}$, while Theorem 4.3 extends the result to the case of an infinite-dimensional biomarker requiring a finite expansion for the possible estimators $\widehat{\beta}$. In Theorem 4.2 below, to strengthen the fact that we are dealing with finite-dimensional observations, the biomarkers and the index coefficient are indicated with boldface.

Theorem 4.2. *Assume that $\mathcal{H} = \mathbb{R}^k$ and let $\{\mathbf{x}_{j,i}\}_{i=1}^{n_j}$, $j = D, H$, be independent observations in \mathbb{R}^k . Let $\widehat{\beta}$ be a strongly consistent estimator of β_0 and assume that $F_{\beta_0,j}$ are continuous for $j = D, H$. Then,*

- a) *Assumption **A3** holds.*
- b) *If in addition $F_{\beta_0,H}$ has density $f_{\beta_0,H}$ such that $f_{\beta_0,H}(u) > 0$, for all $u \in \mathbb{R}$, then the conclusion of Theorem 4.1 holds.*

Let us consider now the situation of a separable Hilbert space, where the estimator $\widehat{\beta}$ is obtained using finite-dimensional candidates obtained from a fixed basis. More precisely, assume that

$$\widehat{\beta} = \sum_{s=1}^k \widehat{b}_s \phi_s, \quad (15)$$

where the coefficients \widehat{b}_s , $s = 1, \dots, k$, are data-dependent and the dimension $k = k_n$ increases with the sample size $n = n_D + n_H$.

Theorem 4.3. Let $\{X_{j,i}\}_{i=1}^{n_j}$, $j = D, H$, be independent observations in a separable Hilbert space \mathcal{H} , let $\widehat{\beta}$ in (15) be an estimator of β_0 such that $\|\widehat{\beta} - \beta_0\| \xrightarrow{a.s.} 0$ and $k_n/n \rightarrow 0$ and assume that $F_{\beta_0,j}$ are continuous for $j = D, H$. Then,

a) Assumption **A3** holds.

b) If in addition $F_{\beta_0,H}$ has density $f_{\beta_0,H}$ such that $f_{\beta_0,H}(u) > 0$, for all $u \in \mathbb{R}$, then the conclusion of Theorem 4.1 holds.

To derive consistency results for the ROC curve associated to $\widehat{\Upsilon}_{\text{QUAD}}$ given in (13), we will consider general quadratic indexes defined as $\Upsilon_{\mathbf{\Lambda}, \boldsymbol{\alpha}}(X) = -\mathbf{x}^\top \mathbf{\Lambda} \mathbf{x} + \boldsymbol{\alpha}^\top \mathbf{x}$ where $\mathbf{x} = A(X) = (\langle X, \phi_1 \rangle, \dots, \langle X, \phi_k \rangle)^\top$, $\boldsymbol{\alpha} \in \mathbb{R}^k$ and $\mathbf{\Lambda} \in \mathbb{R}^{k \times k}$ and $\{\phi_\ell\}_{\ell \geq 1}$ is an orthonormal basis of \mathcal{H} . To avoid complicating the notation, we have omitted the index k related to the number of principal directions chosen which will be assumed to be fixed. As above, we assume that the index Υ used to construct the ROC curve equals $\Upsilon = \Upsilon_{\mathbf{\Lambda}_0, \boldsymbol{\alpha}_0}$ for some squared matrix $\mathbf{\Lambda}_0$ and vector $\boldsymbol{\alpha}_0$. We also assume that estimators $(\widehat{\mathbf{\Lambda}}, \widehat{\boldsymbol{\alpha}})$ of $(\mathbf{\Lambda}_0, \boldsymbol{\alpha}_0)$ are available and that the estimated ROC curve is defined as in (6) through the predictors $\widehat{Y}_{j,i} = \widehat{\Upsilon}(X_{j,i})$, $i = 1, \dots, n_j$, $j = D, H$, where $\widehat{\Upsilon} = \Upsilon_{\widehat{\mathbf{\Lambda}}, \widehat{\boldsymbol{\alpha}}}$. As for the linear index, Assumption **A3** will follow from the consistency of $(\widehat{\mathbf{\Lambda}}, \widehat{\boldsymbol{\alpha}})$.

Again, Assumptions **A1** and **A2** state conditions on the behaviour of the distribution functions $F_j = F_{j, \Upsilon_{\mathbf{\Lambda}_0, \boldsymbol{\alpha}_0}}$ of $Y_j = \Upsilon(X_j) = \Upsilon_{\mathbf{\Lambda}_0, \boldsymbol{\alpha}_0}(X_j)$ which are the usual requirements to establish consistency for univariate biomarkers. Hence, we have the following result.

Theorem 4.4. Let $\{X_{j,i}\}_{i=1}^{n_j}$, $j = D, H$, be independent observations in a separable Hilbert space \mathcal{H} , let $(\widehat{\mathbf{\Lambda}}, \widehat{\boldsymbol{\alpha}})$ be strongly consistent estimators of $(\mathbf{\Lambda}_0, \boldsymbol{\alpha}_0)$ and assume that F_j are continuous. Then,

a) Assumption **A3** holds.

b) If in addition $F_H = F_{H, \Upsilon_{\mathbf{\Lambda}_0, \boldsymbol{\alpha}_0}}$ has density f_H such that $f_H(u) > 0$, for all $u \in \mathbb{R}$, the conclusion of Theorem 4.1 holds.

5 Monte Carlo Study

In this section, we report the results of a numerical study performed with the aim of comparing different rules used to define an estimator of the ROC curve. In particular, we consider the estimators defined through (10) and (14). The estimator defined in (10) may also be used when $\beta(t) = 1$ for all t , which leads to the ROC curve based on the integral-type index labelled $\Upsilon_I(X) = \int_{\mathcal{I}} X(t)dt$. Beyond these discriminating indexes, the maximum and the minimum of each trajectory are also used as discriminating rule, that is, the ROC curve is based on $\Upsilon_{\text{MAX}}(X_{j,i})$ or $\Upsilon_{\text{MIN}}(X_{j,i})$, $i = 1, \dots, n_j$, $j = D, H$, where $\Upsilon_{\text{MAX}}(X) = \max_{t \in \mathcal{I}} X(t)$ and $\Upsilon_{\text{MIN}}(X) = \min_{t \in \mathcal{I}} X(t)$. The operators Υ_I , Υ_{MAX} and Υ_{MIN} used in [Jang and Manatunga \(2022\)](#) do not involve unknown parameters.

In contrast, we include in our simulations some operators that require estimation of population quantities. First, we consider the non-necessarily optimal but natural linear rule defined as $\hat{\Upsilon}_M(X) = \langle \bar{X}_D - \bar{X}_H, X \rangle$ which corresponds to an estimator of the linear discriminating rule based on the mean difference $\Upsilon_M(X) = \langle \mu_D - \mu_H, X \rangle$. Secondly, we consider the estimator of the optimal linear discriminating rule defined in Section 3.2 labelled $\hat{\Upsilon}_{\text{LIN}}(X) = \langle \hat{\beta}, X \rangle$, where the $\hat{\beta}$ is computed as follows. Let $\hat{\Gamma}_A$ be the operator $\hat{\Gamma}_A = (\hat{\Gamma}_D + \hat{\Gamma}_H)/2$ and denote \mathcal{H}_k the linear space spanned by the first k eigenfunctions of the pooled covariance operator $\hat{\Gamma}_{\text{POOL}} = (n_D/n)\hat{\Gamma}_D + (n_H/n)\hat{\Gamma}_H$, related to its largest eigenvalues, with $\hat{\Gamma}_j$ the sample covariance operators of the j -th sample, $j = D, H$ and $n = n_D + n_H$. The estimator $\hat{\beta}$ is obtained by maximizing $\hat{L}(\beta) = \langle \beta, \hat{\mu}_D - \hat{\mu}_H \rangle / \left(\langle \beta, \hat{\Gamma}_A \beta \rangle \right)^{1/2}$, over $\{\beta \in \mathcal{H}_k : \|\beta\| = 1\}$. In all cases, the dimension k is chosen as the smallest dimension ensuring that at least a 95% of the total variability is explained, measured through the eigenvalues of $\hat{\Gamma}_{\text{POOL}}$.

Finally, we also include in the comparison the quadratic discriminating rule $\hat{\Upsilon}_{\text{QUAD}}$ defined in (13). The results for the AUC and ROC curve estimators obtained using each discriminating index are indicated in all Tables and Figures through the considered index. We consider several frameworks including equal or different covariance operators as well as equal or different mean functions.

Sections 5.1 and 5.2 report the obtained results for different Gaussian processes, when differences between mean curves are present and for equal mean functions. For all scenarios, we performed 1000 replications where the trajectories were recorded over a grid of 100 points equally spaced on $[0, 1]$. The estimated ROC curves were computed over a grid of 101 points equally spaced on $[0, 1]$. In Section 5.1, we consider equal sample sizes for both populations, $n_D = n_H = 300$, while Section 5.2 is concerned with an unbalanced design, $n_D = 30$ and $n_H = 250$ and a setting with proportional covariance operators.

5.1 Numerical results for balanced designs

In this section we analyse the performance of the discriminating indexes mentioned above for different Gaussian processes. In all settings $\mu_H(t) = 0$, so that the possible differences between mean functions is given through μ_D , which varies across scenarios. We describe below the different scenarios considered which are labelled **PROP**, **CPC** and **DIFF**.

- **PROP**: This scenario corresponds to the case of proportional covariance operators $\Gamma_D = \rho\Gamma_H$. When $\rho = 1$ it corresponds to the situation of equal covariance operators. In this last setting, the linear discriminating rule \widehat{Y}_{LIN} usually improves the quadratic one in the multivariate setting for different mean functions. We consider the case of equal and different mean functions, that will be labelled **P0** and **P1**.

★ **P0**: Under this setting, $\mu_D(t) = \mu_H(t) = 0$ and $\Gamma_D = \rho\Gamma_H$ with $\rho = 2$.

★ **P1**: In this case, $\mu_D(t) = 2 \sin(\pi t)$ and $\Gamma_D = \rho\Gamma_H$ with $\rho = 1$ and 2.

In these two scenarios both populations have the same underlying Gaussian distribution up to changes in the mean and/or covariance operators.

Two possible Gaussian processes were selected: the Brownian motion and a random Gaussian process with exponential kernel, labelled Exponential Variogram in all Tables and Figures. For the former, covariance kernel for the healthy population equals $\gamma_H(s, t) = \min(s, t)$, while for the latter it corresponds to $\gamma_H(s, t) = \exp(-|s - t|/\theta)$ with $\theta = 0.2$.

- **CPC**: This scenario corresponds to the situation where the covariance operators satisfy a FCPC model. The sample $X_{H,i}$, $i = 1, \dots, n_H$, was generated as a Brownian motion with kernel $\gamma_H(s, t) = \min(s, t)$. Recall that the eigenfunctions of the Brownian covariance operator are $\phi_\ell(t) = \sqrt{2} \sin\{(2\ell - 1)\pi t/2\}$ with related principal values $\lambda_{H,\ell} = 10 [2/\{(2\ell - 1)\pi\}]^2$.

The diseased population is a finite-range one, generated as $X_{D,i} = \mu_D + Z_{1,i}\phi_1 + Z_{2,i}\phi_2 + Z_{3,i}\phi_3$, where $Z_{\ell,i} \sim N(0, \lambda_{D,\ell})$, with two possible choices for the variances of the scores.

- ★ **C1**: In the first one, $\lambda_{D,1} = 2$, $\lambda_{D,2} = 0.3$ and $\lambda_{D,3} = 0.05$. In this situation the order between eigenvalues is preserved across populations.
- ★ **C2**: For the second choice, $\lambda_{D,1} = 0.3$, $\lambda_{D,2} = 2$ and $\lambda_{D,3} = 0.05$. Note that, in this setting, the order between eigenvalues is not preserved, meaning that the vectors $\mathbf{x}_j = (\langle \phi_1, X_{j,1} \rangle, \langle \phi_2, X_{j,1} \rangle, \langle \phi_3, X_{j,1} \rangle)^\top$ will be normally distributed with diagonal covariance matrices $\text{DIAG}(\lambda_{j,1}, \lambda_{j,2}, \lambda_{j,3})$, but the order between the first two principal axes is reversed between populations.

For each of the above described schemes, we allow for two different mean settings. On the one hand, we labelled with a 0 after its identifier, that is, according to the choice of $\lambda_{D,\ell}$, for $\ell = 1, 2, 3$, as **C10** or **C20** the situation where $\mu_D(t) = 0$, for all $t \in (0, 1)$. On the other hand, the cases **C11** or **C21** correspond to the situation where the diseased population has mean $\mu_D(t) = 3 \sin(\pi t)$.

- **DIFF**: We also consider a situation where the processes have different covariance operators and do not share their eigenfunctions. Hence, this framework is not included in the proportional or FCPC models described above. Scheme **DIFF** includes two different settings, but in both of them, the sample $X_{D,i}$, $i = 1, \dots, n_D$, was generated as a Brownian motion with kernel $\gamma_H(s, t) = \min(s, t)$, whereas the sample $X_{H,i}$, $i = 1, \dots, n_H$, was generated as described below.

- ★ **D1**: Under **D1**, the healthy population corresponds to an Ornstein Uhlenbeck process with mean $\mu_H \equiv 0$ and covariance kernel $\gamma_H(s, t) = \{1/(2\theta)\} \exp\{-\theta(s +$

$t\} [\exp\{2\theta(s+t)\} - 1]$, with $\theta = 1/3$.

- ★ **D2**: In this framework, $X_{H,i}$ is distributed as a centered Exponential Variogram, that is, $\gamma_H(s,t) = \exp(-|s-t|/\theta)$ with $\theta = 0.2$ and $\mu_H(t) = 0$, for all t .

As above, we include two different mean scenarios: the one labelled a 0 after its identifier, that is, as **D10** or **D20** corresponds to the situation where $\mu_H(t) = \mu_D(t) = 0$, for all $t \in (0, 1)$. In contrast, the cases **D11** or **D21** correspond to the situation where $\mu_H(t) = 0$ and the diseased population has mean $\mu_D(t) = 2 \sin(\pi t)$.

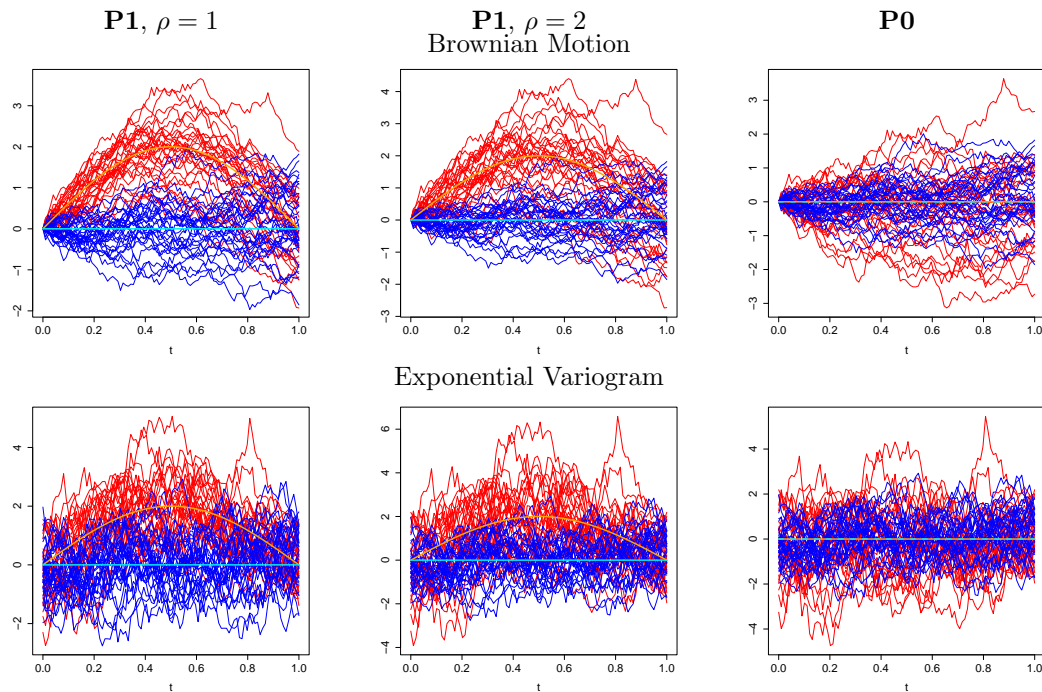


Figure 2: Data sets for proportional models (scheme **PROP**). Blue and red lines correspond to $X_{H,i}$ and $X_{D,i}$, respectively, while the true mean functions μ_H and μ_D are depicted in cyan and orange lines, respectively.

Figures 2 and 3 depict 30 trajectories generated for the healthy and diseased populations in blue and red lines, respectively, under the schemes **PROP** and **CPC**, while Figure 4 displays some of the generated trajectories for each scenario in **DIFF**. Figures 2 and 3 reveal that when $\mu_H = \mu_D = 0$, the differences between the two underlying distributions are more difficult to detect under the proportional model with $\rho = 2$ than under the FCPC model. Under the considered FCPC model, the smoothness and the differences in the range of the trajectories allow

to distinguish the two populations. We do not consider the scheme, $\mu_D(t) = \mu_H(t) = 0$ and $\Gamma_D = \rho \Gamma_H$ with $\rho = 1$, since in this case both populations have the same distribution. For that reason in Table 1 below the cells corresponding to **P0** and $\rho = 1$ are empty. Besides, when both population means are equal, under scenario **D20** the populations may be easily discriminated by looking at their behaviour at $t = 0$, in contrast scheme **D10** seems more challenging.

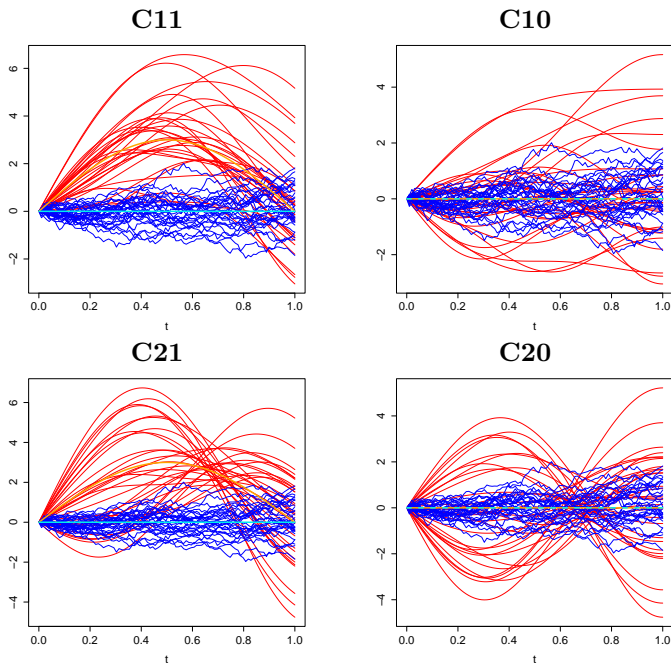


Figure 3: Data sets for under a FCPC model (scheme **CPC**). Blue and red lines correspond to $X_{H,i}$ and $X_{D,i}$, respectively, while the true mean functions μ_H and μ_D are depicted in cyan and orange lines, respectively.

Tables 1 and 2 report the mean and standard deviations over 1000 replications of the AUC estimators under scenarios **PROP** and **CPC**, while Table 3 displays the same summary measures under scenario **DIFF**. To facilitate the reading we indicate in boldface the largest value attained for the mean of the AUC and in italic, the second largest. The obtained results reveal that in all cases, the best performance is obtained by the quadratic rule, $\hat{\Upsilon}_{\text{QUAD}}$, followed in most situations by the linear one induced by the coefficient maximizing $\text{AUC}(\beta)$ as defined in Section 3.1, that is, by $\hat{\Upsilon}_{\text{LIN}}$. It is worth mentioning that under the proportional model when the means of both populations are equal or when means are different but the underlying process is an Exponential Variogram, the rule Υ_{MAX} based on the maximum value of the trajectory achieves a larger mean value of the AUC estimators than $\hat{\Upsilon}_{\text{LIN}}$, a fact that is clearly revealed

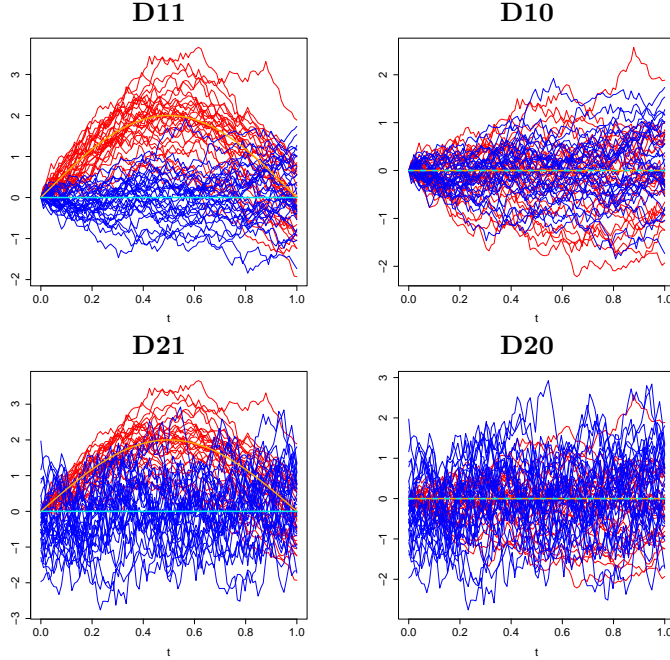


Figure 4: Data sets for under scheme **DIFF**. The left panel corresponds to the case $\mu_H(t) = 0$ and $\mu_D(t) = 3 \sin(\pi t)$ and the right one to $\mu_D(t) = \mu_H(t) = 0$. Blue and red lines correspond to $X_{H,i}$ and $X_{D,i}$, respectively, while the true mean functions μ_H and μ_D are depicted in cyan and orange lines, respectively.

in Figure 5 that presents the boxplots of the AUC estimators. When the mean functions are equal, the discriminating indexes based on a linear rule, Υ_I , $\hat{\Upsilon}_M$ and $\hat{\Upsilon}_{LIN}$, barely exceed an average estimated AUC of 0.5. The rule based on the maximum has a much better performance under **C20** than under **C10**, while under a proportional model with equal means (**P0**), the differences between populations seem to be more easily detected by Υ_{MAX} for the Exponential Variogram process than for the Brownian one.

Figures 5, 6 and 7 present the boxplots of the AUC estimators, under the proportional model, the FCPC one and under scheme **DIFF**, respectively. In particular, Figures 6 and 7 highlight the performance differences as the models vary. It is evident from these plots that scheme **D10** is the more challenging one and only for $\hat{\Upsilon}_{QUAD}$ most estimators are larger than 0.55. There are several simulation scenarios where the obtained AUCs are clearly below 0.5. For example, Υ_{MIN} achieves 0.2823 and 0.2647 under **P0** (Exponential Variogram, $\rho = 2$) and **C20**, respectively. This means in fact that, if the roles of the healthy and diseased populations are interchanged, the corresponding rule would achieve AUCs of $1 - 0.2823$ and $1 - 0.2647$,

Table 1: Mean and standard deviation of the $\widehat{\text{AUC}}$, under scenario **PROP**, that is, under a proportional model $\gamma_D(t, s) = \rho \gamma_H(t, s)$ with equal (**P0**) or different mean functions (**P1**), $\mu_H(t) = 0$ and $\mu_D(t) = 2 \sin(\pi t)$. In all cases, $n_H = n_D = 300$.

ρ		Υ_{MAX}	Υ_{MIN}	Υ_{I}	$\hat{\Upsilon}_{\text{M}}$	$\hat{\Upsilon}_{\text{LIN}}$	$\hat{\Upsilon}_{\text{QUAD}}$	Υ_{MAX}	Υ_{MIN}	Υ_{I}	$\hat{\Upsilon}_{\text{M}}$	$\hat{\Upsilon}_{\text{LIN}}$	$\hat{\Upsilon}_{\text{QUAD}}$
		P1						P0					
Brownian Motion													
1	Mean	0.9520	0.6963	0.9389	0.9653	<i>0.9892</i>	0.9987						
	SD	0.0083	0.0219	0.0094	0.0057	0.0004	0.0007						
2	Mean	0.9434	0.6183	0.8965	0.9309	<i>0.9845</i>	0.9945	<i>0.5977</i>	0.4025	0.4998	0.5307	0.5465	0.7648
	SD	0.0091	0.0237	0.0133	0.0090	0.0017	0.0022	0.0239	0.0233	0.0244	0.0136	0.0165	0.0229
Exponential Variogram													
1	Mean	0.9200	0.7653	0.9426	0.9616	<i>0.9644</i>	0.9809						
	SD	0.0108	0.0191	0.0090	0.0068	0.0051	0.0045						
2	Mean	<i>0.9520</i>	0.5511	0.9011	0.9259	0.9349	0.9905	<i>0.7179</i>	0.2823	0.5000	0.5575	0.6005	0.9627
	SD	0.0082	0.0242	0.0128	0.0107	0.0088	0.0031	0.0212	0.0211	0.0244	0.0134	0.0165	0.0069

Table 2: Mean and standard deviation of the $\widehat{\text{AUC}}$, under scenario **CPC**, which corresponds to processes with different mean functions $\mu_H(t) = 0$ and $\mu_D(t) = 3 \sin(\pi t)$ (**C11** and **C21**) or equal means (**C10** and **C20**). In all cases, $n_H = n_D = 300$.

	Υ_{MAX}	Υ_{MIN}	Υ_{I}	$\hat{\Upsilon}_{\text{M}}$	$\hat{\Upsilon}_{\text{LIN}}$	$\hat{\Upsilon}_{\text{QUAD}}$	Υ_{MAX}	Υ_{MIN}	Υ_{I}	$\hat{\Upsilon}_{\text{M}}$	$\hat{\Upsilon}_{\text{LIN}}$	$\hat{\Upsilon}_{\text{QUAD}}$
$\lambda_D = (2, 0.30, 0.05)^\top$												
	C11						C10					
Mean	0.9417	0.6103	0.9099	0.9417	<i>0.9853</i>	0.9905	0.5248	0.4723	0.4985	0.5266	<i>0.5291</i>	0.8531
SD	0.0101	0.0257	0.0132	0.0093	0.0049	0.0038	0.0248	0.0253	0.0247	0.0154	0.0174	0.0160
$\lambda_D = (0.30, 2, 0.05)^\top$												
	C21						C20					
Mean	<i>0.9922</i>	0.5355	0.9856	0.9810	0.9881	0.9966	<i>0.7340</i>	0.2647	0.4991	0.5296	0.5295	0.9090
SD	0.0024	0.0250	0.0036	0.0046	0.0031	0.0013	0.0214	0.0207	0.0239	0.0166	0.0166	0.0126

respectively. These values are similar to the ones of Υ_{MAX} under the same simulation scenarios. Analogous comments can be done for Υ_{MAX} under **D20**, which yields an AUC of 0.1486. In summary, in most scenarios, the quadratic rule outperforms the considered competitors.

To visualize the performance of the different estimators of the ROC curve, we used the functional boxplots, as defined in Sun and Genton (2011). The functional boxplots of the $n_R = 1000$ realizations of the different estimators of the ROC curve under models **P0** and **P1** with $\rho = 2$ are displayed in Figures 8 and 9. In these plots, the magenta central box

Table 3: Mean and standard deviation of the $\widehat{\text{AUC}}$, under scenario **DIFF**, when different covariance operators are considered. Under **D11** and **D21**, $\mu_H(t) = 0$ and $\mu_D(t) = 2 \sin(\pi t)$, while for the schemes **D10** and **D20** $\mu_D = \mu_H \equiv 0$. In all cases, $n_H = n_D = 300$.

	Υ_{MAX}	Υ_{MIN}	Υ_{I}	$\widehat{\Upsilon}_{\text{M}}$	$\widehat{\Upsilon}_{\text{LIN}}$	$\widehat{\Upsilon}_{\text{QUAD}}$		Υ_{MAX}	Υ_{MIN}	Υ_{I}	$\widehat{\Upsilon}_{\text{M}}$	$\widehat{\Upsilon}_{\text{LIN}}$	$\widehat{\Upsilon}_{\text{QUAD}}$
	D11							D10					
Mean	0.9607	0.6956	0.9454	<i>0.9695</i>	0.9988	0.9988	0.5048	0.4953	0.4996	0.5314	<i>0.5486</i>	0.5989	
SD	0.0072	0.0221	0.0088	0.0053	0.0007	0.0007	0.0244	0.0238	0.0242	0.0130	0.0163	0.0187	
	D21							D20					
Mean	0.7370	0.9123	0.9407	0.9634	<i>0.9844</i>	1.0000	0.1486	0.8512	0.4996	0.5491	<i>0.5864</i>	1.0000	
SD	0.0207	0.0118	0.0092	0.0064	0.0042	0.0000	0.0154	0.0159	0.0242	0.0140	0.0180	0.0002	

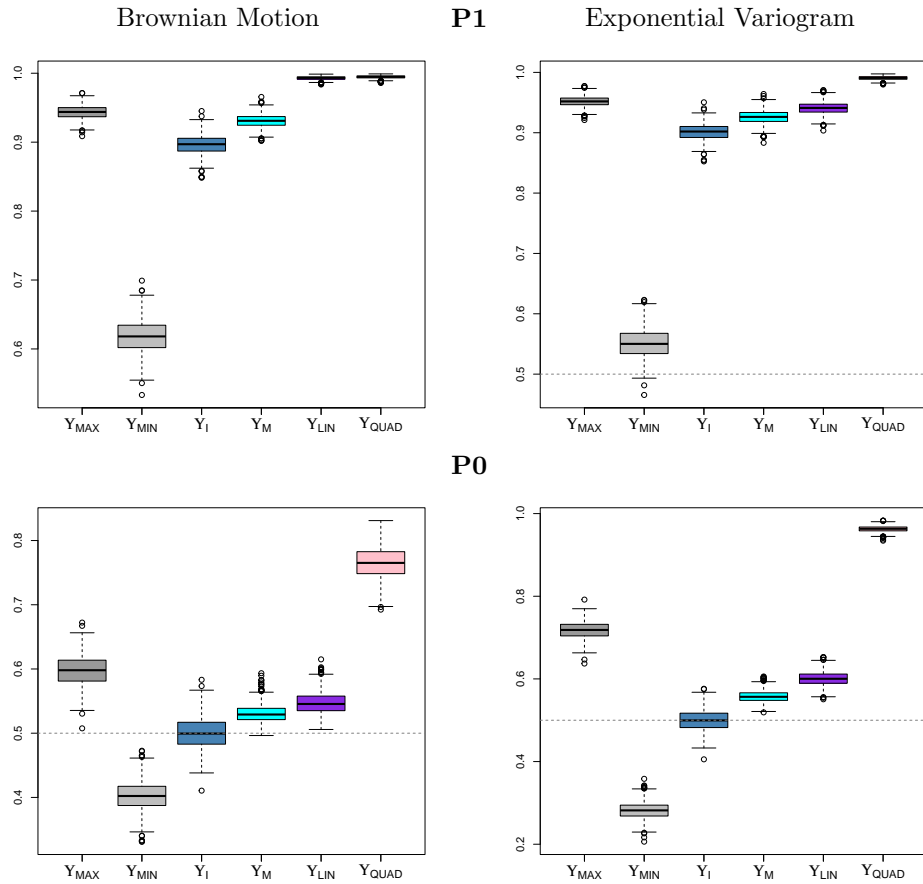


Figure 5: Boxplots of the estimators of the AUC under scenario **PROP** with $\rho = 2$. The horizontal dashed line, when appearing, indicates 0.5.

represents the 50% inner band of curves, the solid black line indicates the central (deepest) function and the dotted red lines indicate outlying curves (in this case: outlying estimates $\widehat{\text{ROC}}_j$ for some $1 \leq j \leq 1000$). The blue lines correspond to the envelopes, that is, the whiskers

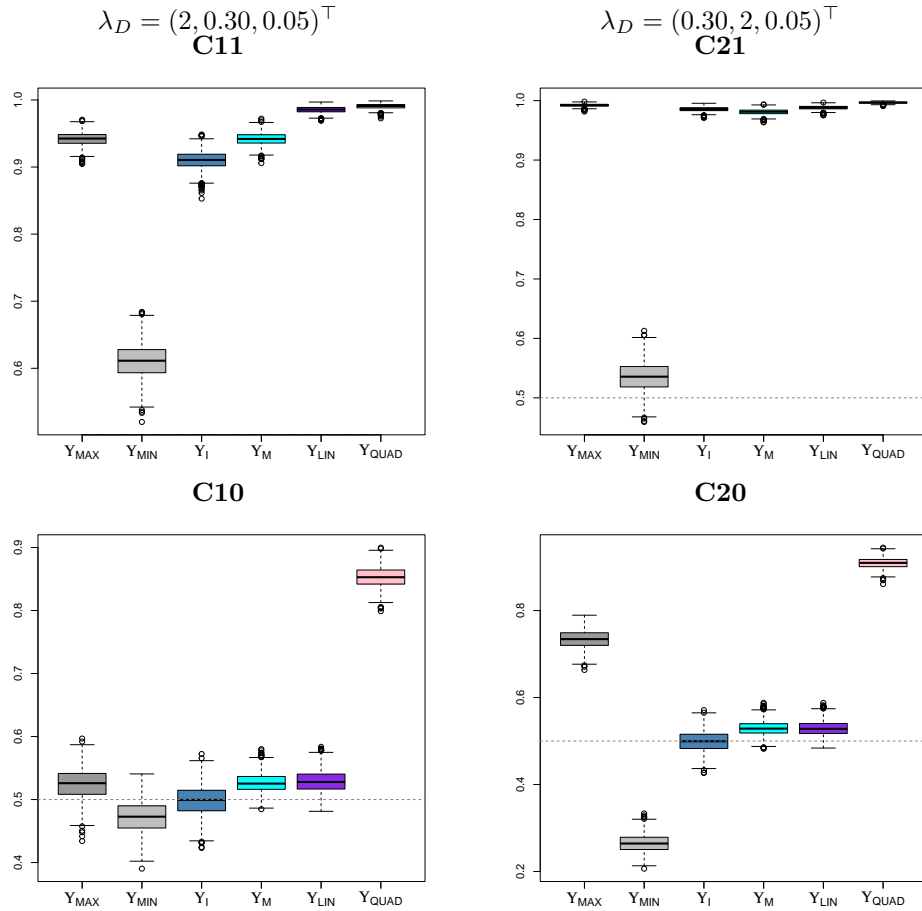


Figure 6: Boxplots of the estimators of the AUC under scenario **CPC**. The horizontal dashed line, when appearing, indicates 0.5.

in the univariate boxplot and demarcate the limits for a curve to be identified as atypical. The diagonal, in gold color, is shown for comparison purposes. Similarly, Figures 10 and 11 display the functional boxplots under the FCPC model and Figures 12 and 13 depict the corresponding ones under schemes **D1** and **D2**, respectively. We do not show the results for Υ_{MIN} since it corresponds to the procedure with the worst performance.

The behaviour observed in the functional boxplots is consistent with that of the AUC estimators. When the populations have equal mean, for the linear indexes, Υ_I , $\hat{\Upsilon}_M$ and $\hat{\Upsilon}_{\text{LIN}}$, the central region containing the 50% deepest ROC curve estimators includes or crosses the identity function, except under the proportional model when considering the Exponential Variogram where the ROC curve estimators associated to $\hat{\Upsilon}_M$ and $\hat{\Upsilon}_{\text{LIN}}$ exceed the diagonal for values of p smaller than 0.4. The worst scenarios for these rules seem to be the FCPC model under **C10**,

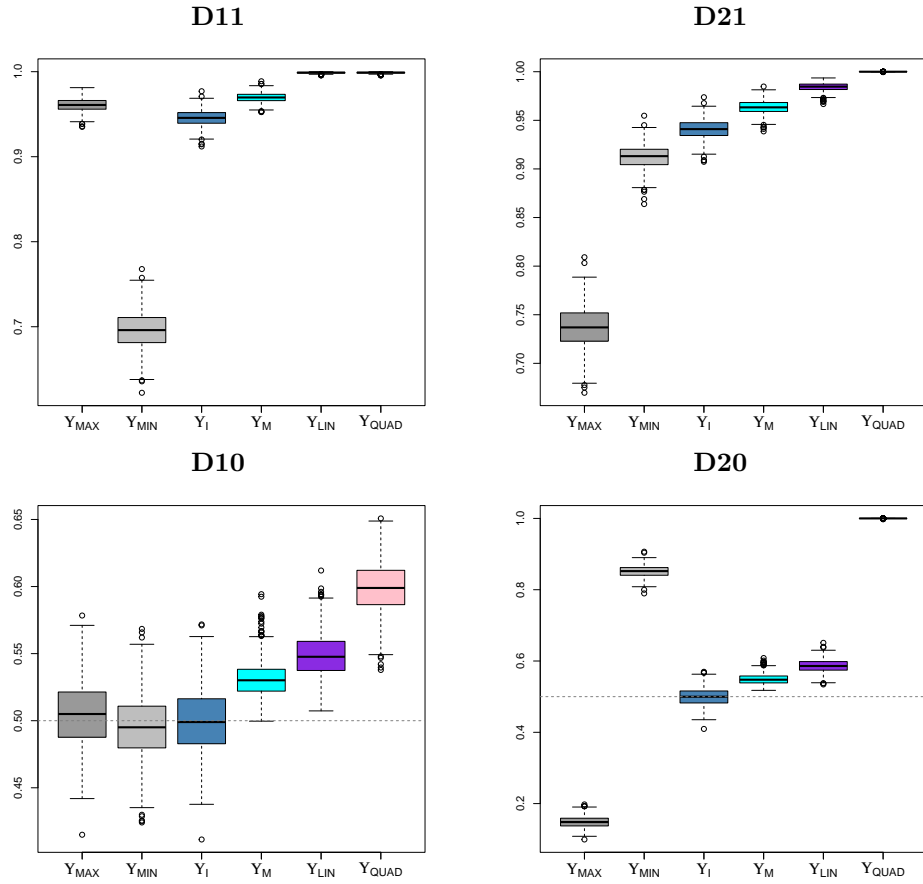


Figure 7: Boxplots of the estimators of the AUC under scheme **DIFF**. The horizontal dashed line, when appearing, indicates 0.5.

when $\lambda_D = (2, 0.30, 0.05)^\top$, and under scheme **D20** for which X_D follows a Brownian motion and X_H an Exponential Variogram. The quadratic index results in the best discriminating index for the considered simulation schemes, providing a perfect rule under **D2**.

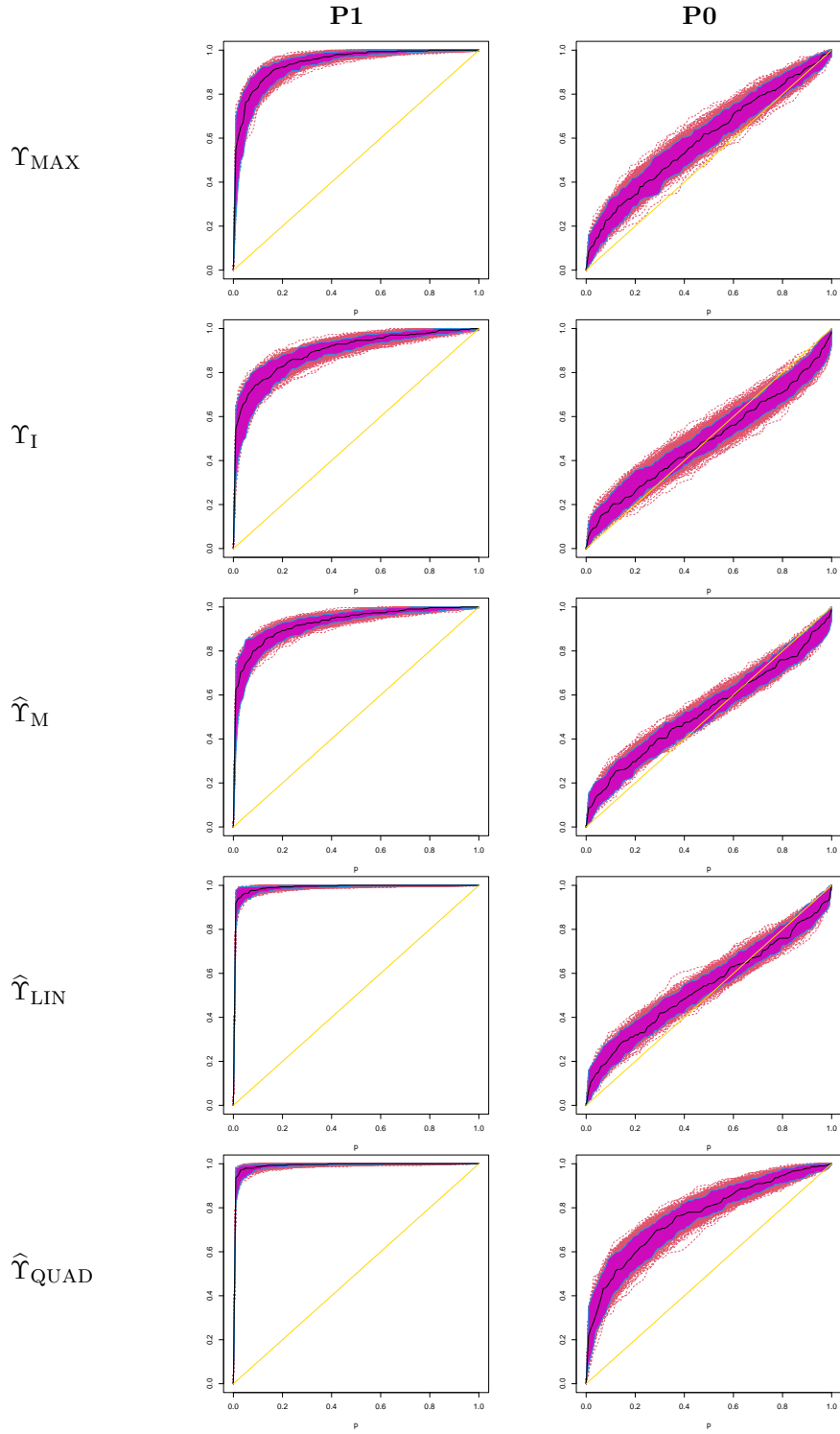


Figure 8: Functional boxplots of the estimators $\widehat{\text{ROC}}$ under scenario **PROP** with $\rho = 2$ for the Brownian motion setting. Rows correspond to discriminating indexes, while columns to $\mu_D(t) = 2 \sin(\pi t)$ and $\mu_H = 0$.

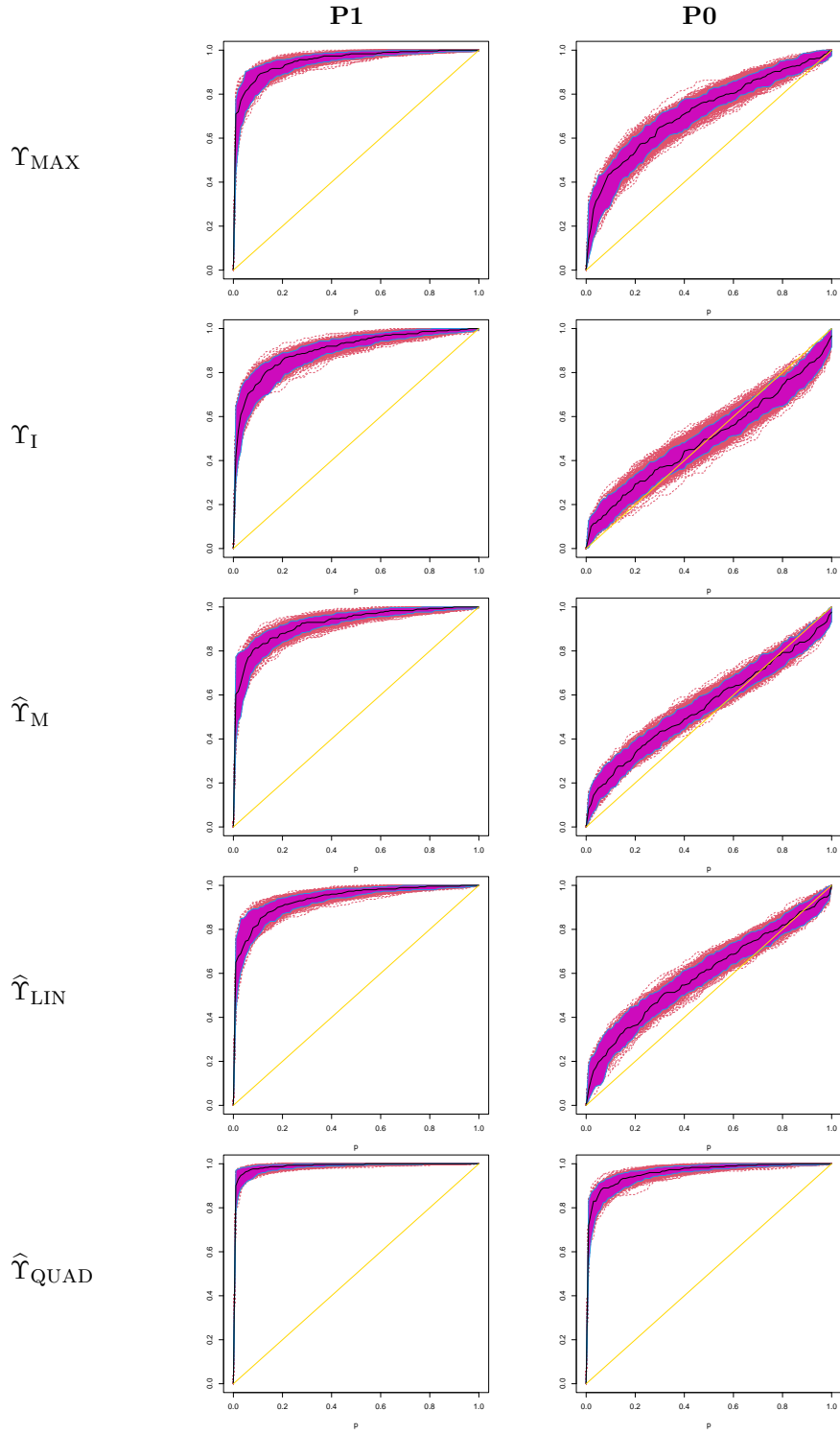


Figure 9: Functional boxplots of the estimators \widehat{ROC} under scenario **PROP** with $\rho = 2$ for the Exponential Variogram process. Rows correspond to discriminating indexes, while columns to $\mu_D(t) = 2 \sin(\pi t)$ and $\mu_H = 0$.

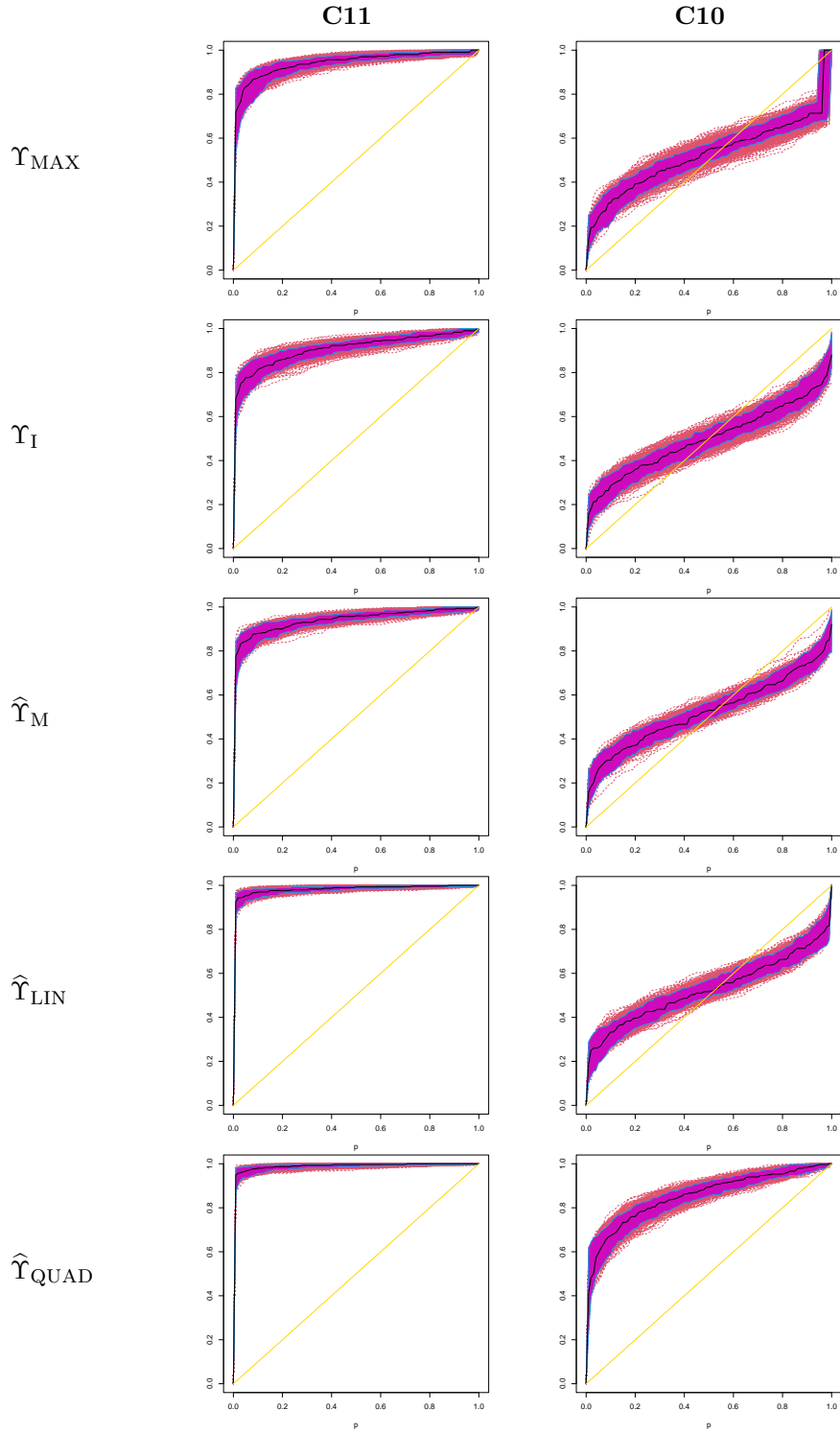


Figure 10: Functional boxplots of the estimators $\widehat{\text{ROC}}$ under a FCPC model with $\lambda_{D,1} = 2$, $\lambda_{D,2} = 0.3$ and $\lambda_{D,3} = 0.05$. Rows correspond to discriminating indexes, while columns to $\mu_D(t) = 2 \sin(\pi t)$ and $\mu_H = 0$.

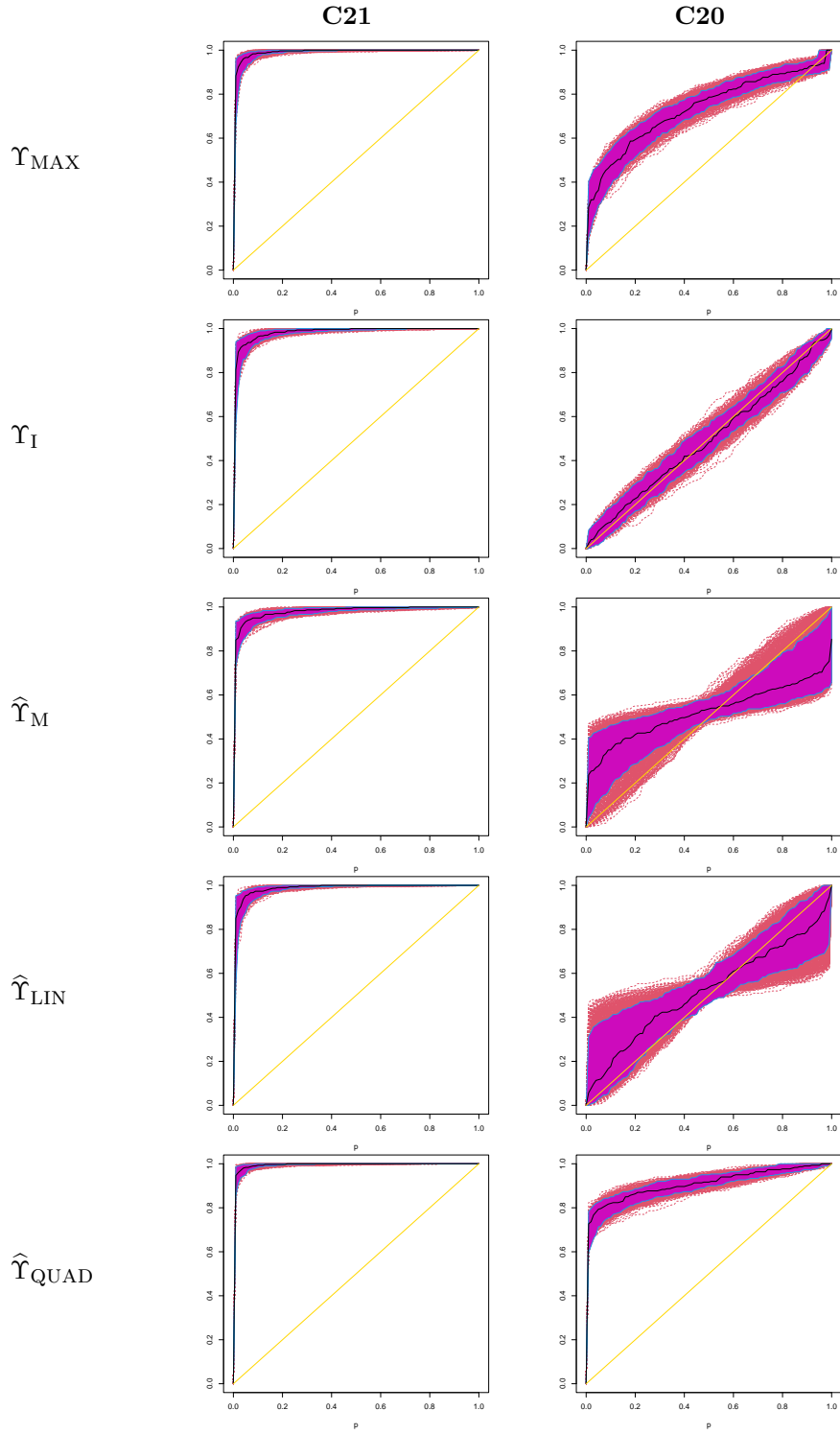


Figure 11: Functional boxplots of the estimators $\widehat{\text{ROC}}$ under a FCPC model with $\lambda_{D,1} = 0.3$, $\lambda_{D,2} = 2$ and $\lambda_{D,3} = 0.05$. Rows correspond to discriminating indexes, while columns to $\mu_D(t) = 2 \sin(\pi t)$ and $\mu_H = 0$.

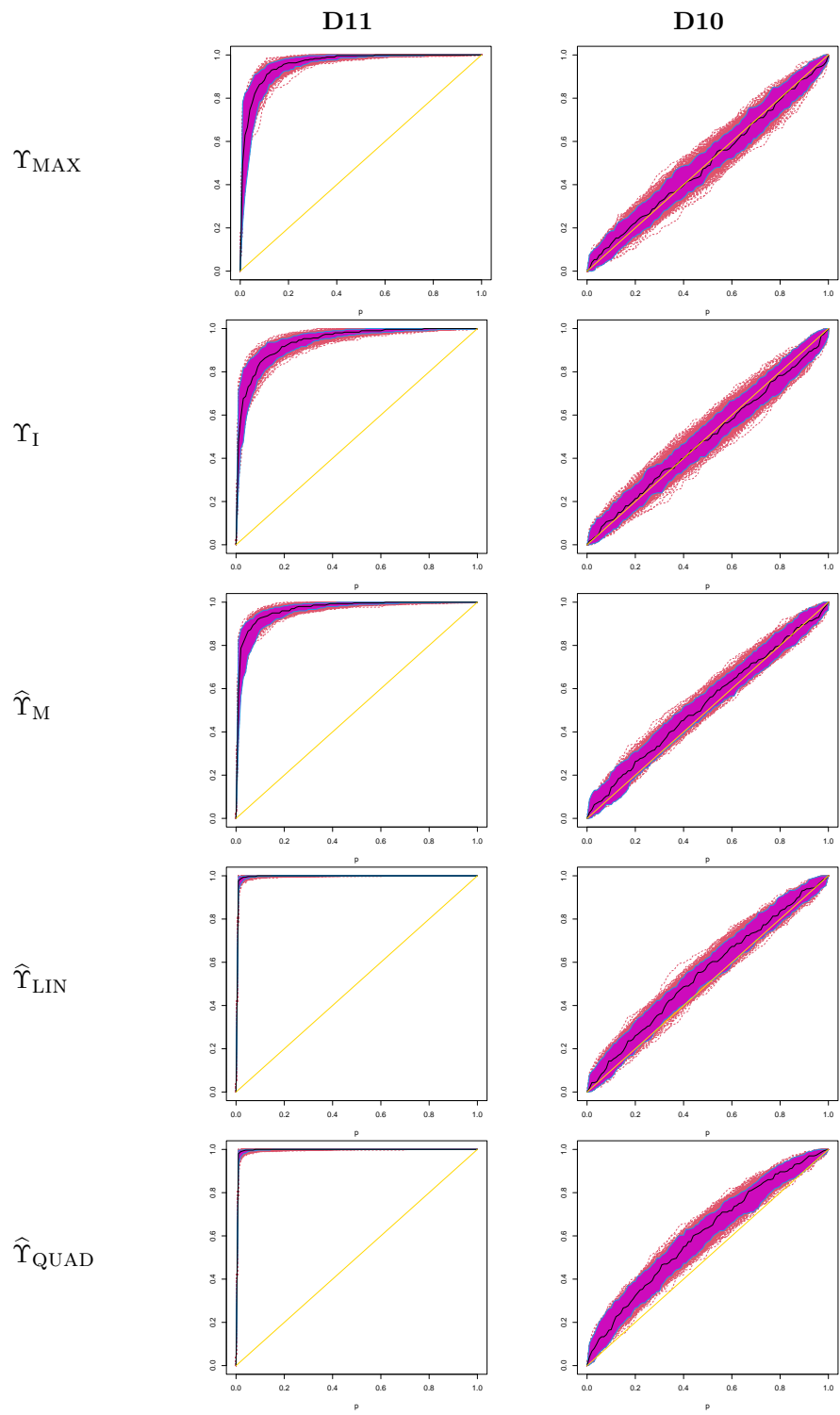


Figure 12: Functional boxplots of the estimators \widehat{ROC} under scheme **D1**. Rows correspond to discriminating indexes, while columns to $\mu_D(t) = 2 \sin(\pi t)$ and $\mu_H = 0$.

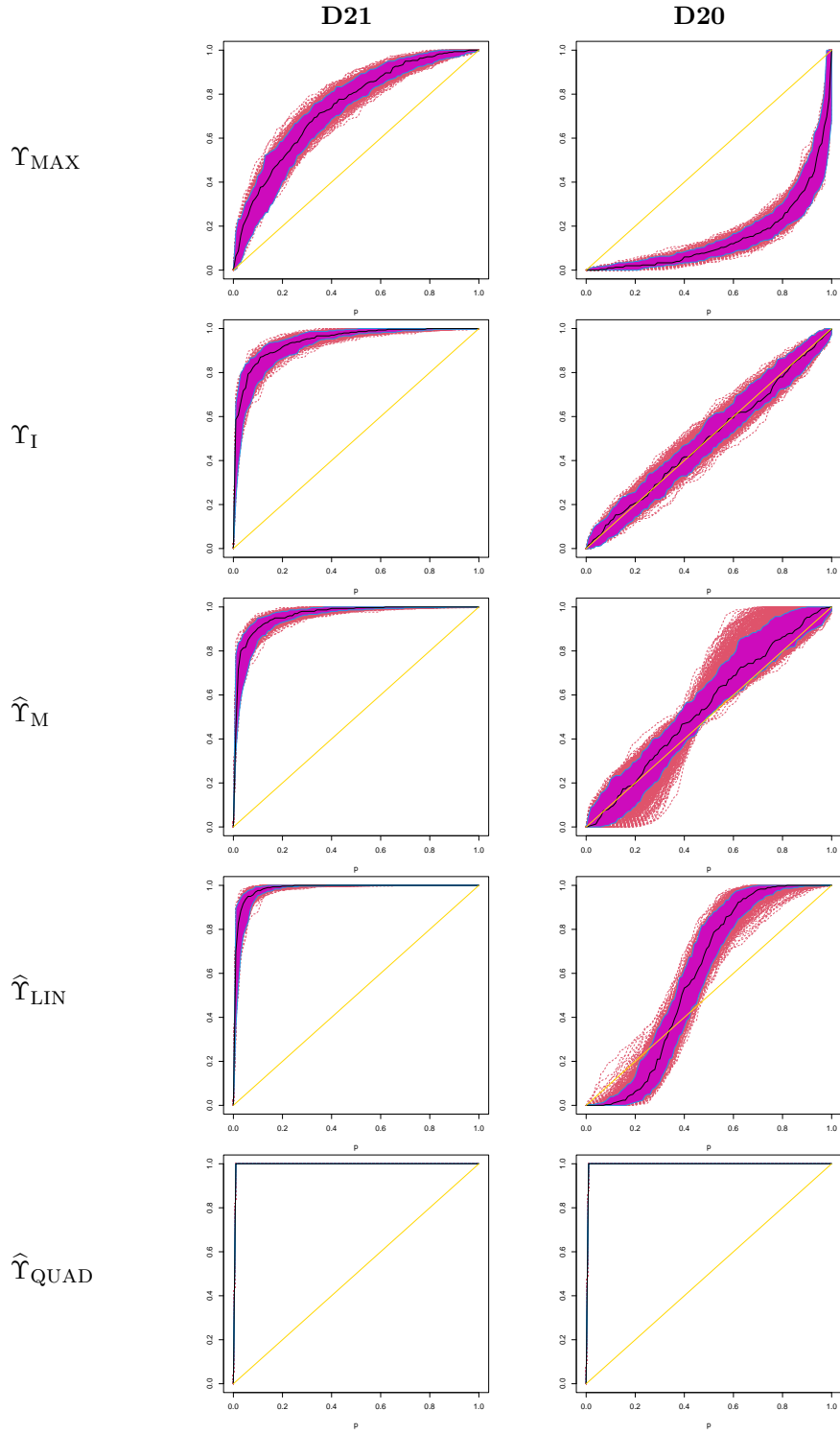


Figure 13: Functional boxplots of the estimators \widehat{ROC} under scheme **D2**. Rows correspond to discriminating indexes, while columns to $\mu_D(t) = 2 \sin(\pi t)$ and $\mu_H = 0$.

5.2 Numerical results for unbalanced designs

In this Section, we report the results of a numerical study conducted to evaluate the effect of unbalanced sample sizes. To consider a framework similar to the cardiotoxicity data set, we chose $n_D = 30$ and $n_H = 250$ under a proportional model with $\rho = 2$. Table 4 displays the mean and standard deviations of the AUC estimators, while Figures 14 and 15 display the functional boxplots corresponding to the estimates of the ROC. The obtained results reveal that, as for the situation where the two samples have the same size, the quadratic rule $\hat{\Upsilon}_{\text{QUAD}}$ outperforms the other competitors, even when this setting is not so harmful for the linear rule as the one where the covariance operators follow a functional common principal component model. This suggests that the quadratic rule should be taken into account in frameworks where equality of the covariance operators may be doubtful.

Table 4: Mean and standard deviation of the $\widehat{\text{AUC}}$, under scenario **PROP**, that is, under a proportional model $\gamma_D(t, s) = \rho \gamma_H(t, s)$ with equal (**P0**) or different mean functions (**P1**), $\mu_H(t) = 0$ and $\mu_D(t) = 2 \sin(\pi t)$. In all cases, $n_H = 250$ and $n_D = 30$.

ρ		Υ_{MAX}	Υ_{MIN}	Υ_{I}	$\hat{\Upsilon}_{\text{M}}$	$\hat{\Upsilon}_{\text{LIN}}$	$\hat{\Upsilon}_{\text{QUAD}}$	Υ_{MAX}	Υ_{MIN}	Υ_{I}	$\hat{\Upsilon}_{\text{M}}$	$\hat{\Upsilon}_{\text{LIN}}$	$\hat{\Upsilon}_{\text{QUAD}}$
P1							P0						
Brownian Motion													
2	Mean	0.9435	0.6187	0.8965	0.9330	<i>0.9937</i>	0.9951	0.5986	0.4031	0.5005	0.5816	<i>0.6216</i>	0.7917
	SD	0.0212	0.0655	0.0346	0.0235	0.0067	0.0057	0.0585	0.0581	0.0635	0.0370	0.0458	0.0462
Exponential Variogram													
2	Mean	0.9521	0.5520	0.9011	0.9295	<i>0.9683</i>	0.9988	0.7193	0.2828	0.5006	0.6518	<i>0.7670</i>	0.9943
	SD	0.0223	0.0658	0.0342	0.0274	0.0173	0.0017	0.0557	0.0546	0.0637	0.0363	0.0402	0.0052

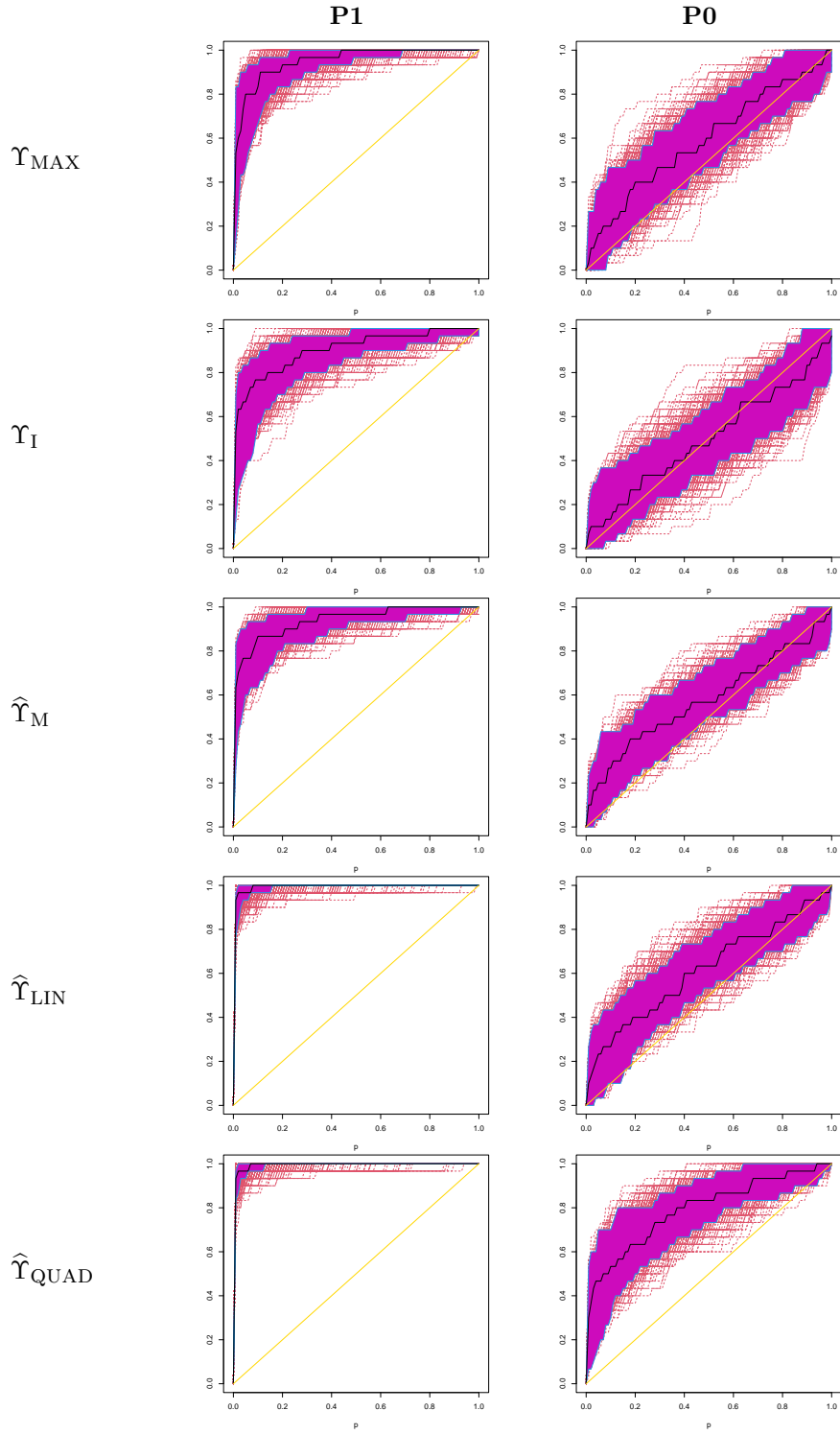


Figure 14: Functional boxplots of the estimators $\widehat{\text{ROC}}$ under scenario **PROP** with $\rho = 2$ for the Brownian motion setting. Rows correspond to discriminating indexes, while columns to $\mu_D(t) = 2 \sin(\pi t)$ and $\mu_H = 0$. The sample sizes are $n_D = 30$ and $n_H = 250$.

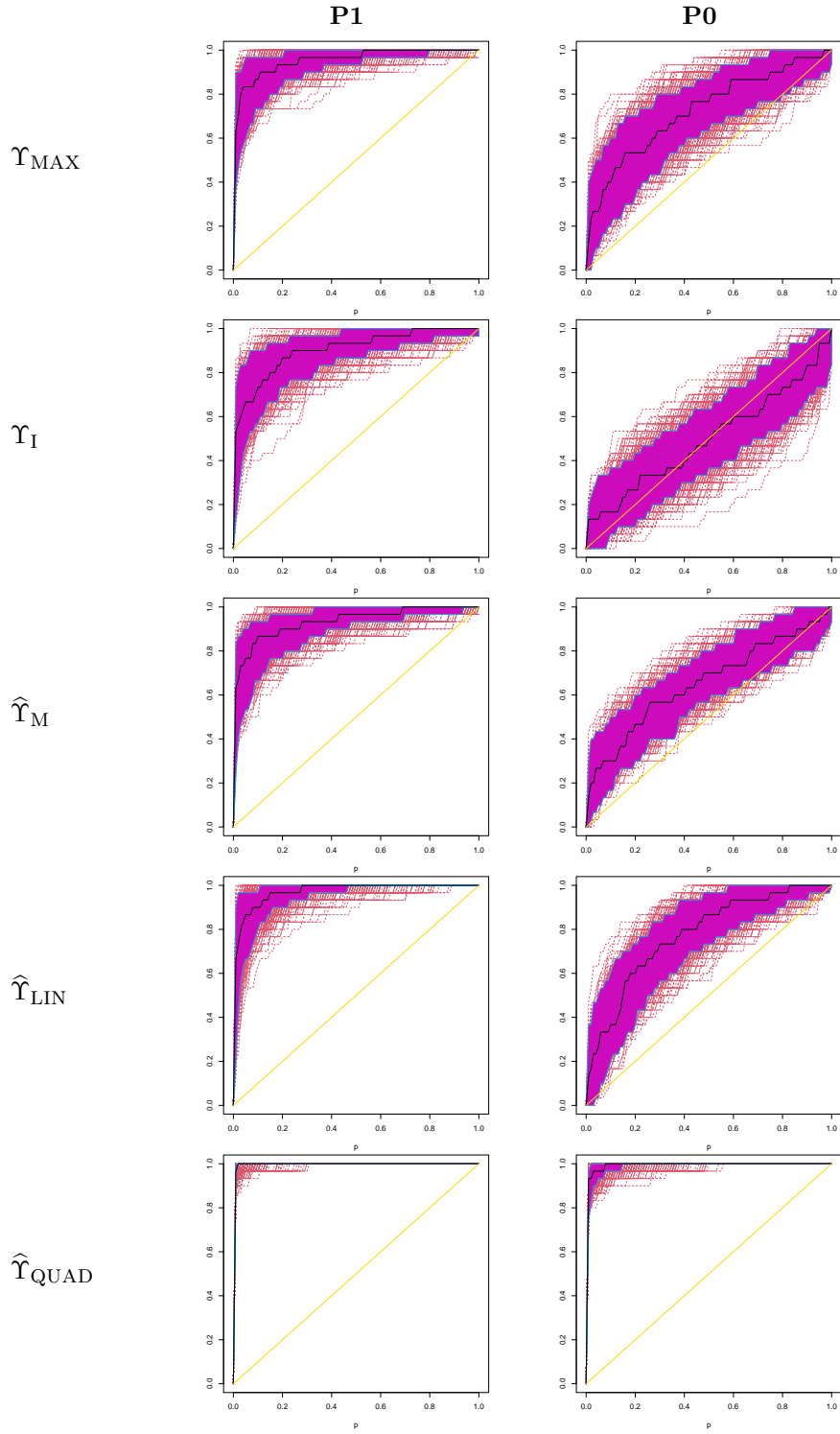


Figure 15: Functional boxplots of the estimators $\widehat{\text{ROC}}$ under scenario **PROP** with $\rho = 2$ for the Exponential Variogram process. Rows correspond to discriminating indexes, while columns to $\mu_D(t) = 2 \sin(\pi t)$ and $\mu_H = 0$. The sample sizes are $n_D = 30$ and $n_H = 250$.

6 Real dataset analysis

We illustrate the application of the developed methodology to a real dataset reported in [Piñeiro-Lamas et al. \(2023\)](#) related to the study of cardiotoxicity in breast cancer patients mentioned in the Introduction.

Breast cancers related to high levels of the protein human epidermal growth factor receptor 2 (HER2) are much more likely to respond to treatments with drugs that target the HER2 protein. In fact, therapies that aim specifically HER2 have a strong anti-tumoral effect, improving the overall response of the patient and therefore, the survival expectancy. However, this kind of therapies may have side effects such as cardiotoxicity. In this context, the detection of the cancer therapy-related cardiac dysfunction (CTRCD) is relevant with respect to the prognosis and hence, it is recommended to follow-up the appearance of CTRCD through cardiac imaging tests, among other clinical tests. The availability of good markers to predict CTRCD is important to prevent cardiac problems. The Tissue Doppler Imaging (TDI) is an echocardiographic technique that shows the velocity of myocardial motion. It may be helpful to early identify CTRCD if a study of the heart condition is performed before treatment. TDI shows velocity as a function of time, thus it may be preprocessed to obtain a functional datum, see [Piñeiro-Lamas et al. \(2023\)](#) for more details.

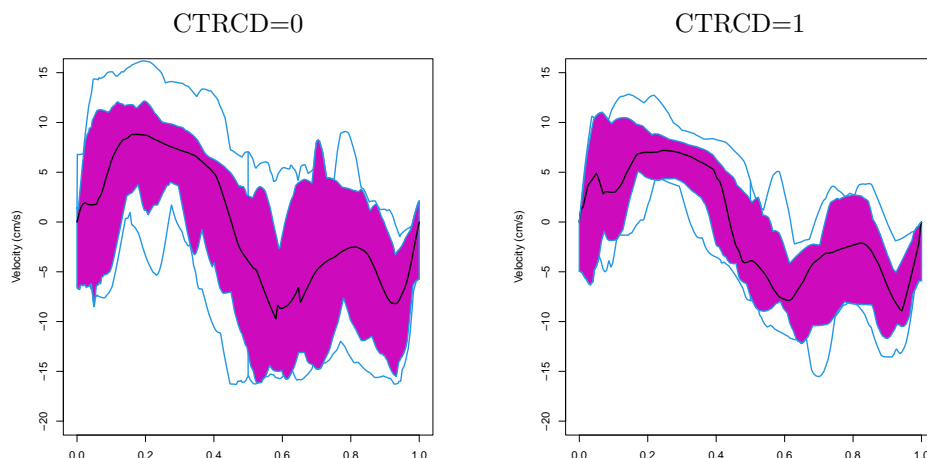


Figure 16: Cardiotoxicity data. Left panel corresponds to the functional boxplot of the cycles of patients without CTRCD, while the right one to women with CTRCD.

The data, displayed in Figure 1, correspond to 270 women diagnosed with HER2+ breast cancer, 27 of them suffer from CTRCD. For each patient the cycle extracted from the TDI discretized in 1001 equispaced points in the interval $[0,1]$ is registered together with their CTRCD status. To have a deeper insight of the cycles in each status of CTRCD, in Figure 16 we display the functional boxplot of each group. No outlying cycles were detected in either group.

Table 5: Cardiotoxicity data. Estimated AUC of each method.

Υ_{MAX}	Υ_{MIN}	Υ_{I}	$\hat{\Upsilon}_{\text{M}}$	$\hat{\Upsilon}_{\text{LIN}}$	$\hat{\Upsilon}_{\text{QUAD}}$
0.4547	0.6770	0.5328	0.6819	0.7034	0.8877

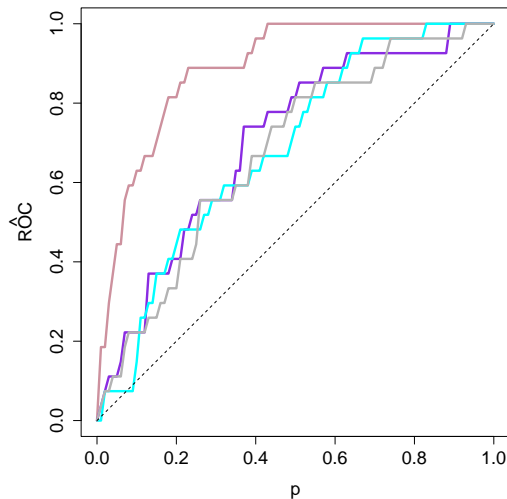


Figure 17: Cardiotoxicity data. Estimated ROC curves with $\text{AUC} \geq 0.65$. The dark pink, violet, cyan and gray lines correspond to the estimators related to the quadratic method, the linear rule, the procedure based on the difference of means and the one based on the minimum, respectively.

In order to assess the performance of the functional biomarker to distinguish between the two categories of CTRCD, we apply the discriminating indexes described in the previous sections. We computed the indexes based on the minimum (Υ_{MIN}), the maximum (Υ_{MAX}), the integral (Υ_{I}), the difference of means ($\hat{\Upsilon}_{\text{M}}$), and the linear ($\hat{\Upsilon}_{\text{LIN}}$) and the quadratic ($\hat{\Upsilon}_{\text{QUAD}}$) criteria taking the number of components that explain at least 95% of the variability, which in this data is attained for $k = 11$. Table 5 collects the AUC for each method. In Figure 17 the estimates of the ROC curve with AUC greater or equal to 0.65 are depicted. The estimator obtained from

the quadratic method is plotted in dark pink, in violet the one corresponding to the linear rule, in cyan the estimate based on the difference of means and in gray that related to the minimum. It is evident from this figure that the better performance is achieved for the quadratic method. The better discriminating capability of the quadratic method is in some sense expectable due to the particular structure of the data, which makes difficult to distinguish the groups just taking into account either the minimum or the maximum or any linear rule.

7 Final Comments

In this paper, in order to construct a suitable ROC curve, we address the problem of defining proper univariate indexes when functional biomarkers are used to distinguish between two populations. The defined indexes allow to construct a ROC curve to measure their discriminating capability. One of our goals was to provide a thorough insight of the difficulties arising at population level to define and estimate a proper ROC curve in the functional setting. In particular, we have discussed the limitations of considering fully known operators to define the discriminant index and to solve this problem we have introduced two methods that require estimation of some unknown parameters. In particular, we have proposed a linear index with the property of maximizing the AUC, when both populations have the same covariance operator. In order to estimate it and to circumvent the curse of dimensionality we have suggested to use either a sieve or a penalized approach. The situation of different covariance structures has been also contemplated by means of a quadratic rule constructed projecting the data over a finite-dimensional space. As discussed in Section 3.3, the need of this finite-dimensional approximation is justified by the fact that the limiting operator is defined only over the intersection of the squared-root covariance operator ranges.

Consistency results for the estimators of the ROC curve and its related summary measures were derived for both linear and quadratic discriminating indexes, under general assumptions. The results of our numerical experiments illustrate the advantages of using a quadratic rule in presence of different covariance operators. The application of our proposals to a real data set

confirms that, when differences between populations arise in covariances more than between means, as revealed in Figure 1, the quadratic index outperforms the linear one and the indexes constructed from known operators.

8 Appendix: Proofs

8.1 Proof of the results in Section 2.2

Proof of (3). To derive (3), first note that the value c maximizing $\Delta_{\beta}(c)$ equals

$$c_{\beta} = \frac{\boldsymbol{\beta}^{\top}(\boldsymbol{\mu}_D + \boldsymbol{\mu}_H)}{2},$$

giving the following expression for the Youden index

$$\begin{aligned} \text{YI}(\boldsymbol{\beta}) &= \left| \Phi \left\{ \frac{\boldsymbol{\beta}^{\top}(\boldsymbol{\mu}_H - \boldsymbol{\mu}_D)}{2(\boldsymbol{\beta}^{\top}\boldsymbol{\Sigma}\boldsymbol{\beta})^{1/2}} \right\} - \Phi \left\{ \frac{\boldsymbol{\beta}^{\top}(\boldsymbol{\mu}_D - \boldsymbol{\mu}_H)}{2(\boldsymbol{\beta}^{\top}\boldsymbol{\Sigma}\boldsymbol{\beta})^{1/2}} \right\} \right| = \left| 1 - 2\Phi \left\{ \frac{\boldsymbol{\beta}^{\top}(\boldsymbol{\mu}_D - \boldsymbol{\mu}_H)}{2(\boldsymbol{\beta}^{\top}\boldsymbol{\Sigma}\boldsymbol{\beta})^{1/2}} \right\} \right| \\ &= \left| 1 - 2\Phi \left\{ \frac{1}{\sqrt{2}}L(\boldsymbol{\beta}) \right\} \right|. \end{aligned}$$

To simplify the notation let $\sigma_{\beta}^2 = \boldsymbol{\beta}^{\top}\boldsymbol{\Sigma}\boldsymbol{\beta}$ and $\boldsymbol{\mu} = (\boldsymbol{\mu}_D - \boldsymbol{\mu}_H)/2$. Then,

$$\text{YI}(\boldsymbol{\beta}) = \left| 1 - 2\Phi \left(\frac{\boldsymbol{\beta}^{\top}\boldsymbol{\mu}}{\sigma_{\beta}} \right) \right|.$$

Taking into account that multiplying $\boldsymbol{\beta}$ by a constant does not change the value of the Youden index, to maximize it, we can search for the maximum of $\text{YI}^2(\boldsymbol{\beta})$ under the constraint that $\sigma_{\beta}^2 = 1$. Let

$$H(\boldsymbol{\beta}) = \{1 - 2\Phi(\boldsymbol{\beta}^{\top}\boldsymbol{\mu})\}^2 + \lambda(\sigma_{\beta}^2 - 1).$$

Then, if $\varphi = \Phi'$, we get that

$$\frac{\partial H}{\partial \boldsymbol{\beta}} = -4 \{1 - 2\Phi(\boldsymbol{\beta}^{\top}\boldsymbol{\mu})\} \varphi(\boldsymbol{\beta}^{\top}\boldsymbol{\mu}) \boldsymbol{\mu} + 2\lambda\boldsymbol{\Sigma}\boldsymbol{\beta}. \quad (\text{A.1})$$

Multiplying (A.1) by β^\top and using that the value maximizing $H(\beta)$ has null gradient and that $\sigma_\beta^2 = 1$, we obtain that

$$\begin{aligned} 0 &= -4 \{1 - 2\Phi(\beta^\top \mu)\} \varphi(\beta^\top \mu) \beta^\top \mu + 2\lambda \beta^\top \Sigma \beta \\ &= -4 \{1 - 2\Phi(\beta^\top \mu)\} \varphi(\beta^\top \mu) \beta^\top \mu + 2\lambda, \end{aligned}$$

which entails that

$$2\lambda = 4 \{1 - 2\Phi(\beta^\top \mu)\} \varphi(\beta^\top \mu) \beta^\top \mu. \quad (\text{A.2})$$

Therefore, if $\beta^\top \mu = 0$, we have that $\lambda = 0$, $\mathbf{0} = \partial H / \partial \beta$ and $H(\beta) = \mathbf{0}$ meaning that the maximum is not reached in directions orthogonal to μ .

Assume that $\beta^\top \mu \neq 0$ and let $\nu_\beta = 4 \{1 - 2\Phi(\beta^\top \mu)\} \varphi(\beta^\top \mu) \neq 0$. Using (A.2), we conclude that $2\lambda = \nu_\beta \beta^\top \mu$. Besides, taking into account that at any critical point $\partial H / \partial \beta = \mathbf{0}$, from (A.1) we conclude that $2\lambda \Sigma \beta = 4 \{1 - 2\Phi(\beta^\top \mu)\} \varphi(\beta^\top \mu) \mu = \nu_\beta \mu$, so

$$\nu_\beta \beta^\top \mu \Sigma \beta = \nu_\beta \mu,$$

or equivalently, $(\beta^\top \mu) \Sigma \beta = \mu$. Denoting $a_\beta = \beta^\top \mu \neq 0$, we have

$$\beta = \Sigma^{-1} \mu \frac{1}{a_\beta},$$

which leads to $a_\beta^2 = \mu^\top \Sigma^{-1} \mu$ and $\beta = \Sigma^{-1} \mu / (\mu^\top \Sigma^{-1} \mu)^{1/2}$, concluding the proof. ■

8.2 Proof of the results in Section 3

Proof of Lemma 3.1. a) Note that as in the multivariate setting

$$\begin{aligned}
\text{Cov}(\langle \beta, X \rangle, G) &= \mathbb{E}(G \langle \beta, X \rangle) - \mathbb{E}\langle \beta, X \rangle \mathbb{E}G = \mathbb{E}\{G \mathbb{E}(\langle \beta, X \rangle | G)\} - \pi_D \mathbb{E}\{\mathbb{E}(\langle \beta, X \rangle | G)\} \\
&= \pi_D \mathbb{E}(\langle \beta, X \rangle | G = 1) - \pi_D \{\pi_D \mathbb{E}(\langle \beta, X \rangle | G = 1) + \pi_H \mathbb{E}(\langle \beta, X \rangle | G = 0)\} \\
&= \pi_D [\mathbb{E}(\langle \beta, X_D \rangle) - \{\pi_D \mathbb{E}(\langle \beta, X_D \rangle) + \pi_H \mathbb{E}(\langle \beta, X_H \rangle)\}] \\
&= \pi_D \{\langle \beta, \mu_D \rangle - (\pi_D \langle \beta, \mu_D \rangle + \pi_H \langle \beta, \mu_H \rangle)\} = \pi_D (\pi_H \langle \beta, \mu_D \rangle - \pi_H \langle \beta, \mu_H \rangle) \\
&= \pi_D \pi_H \langle \beta, \mu_D - \mu_H \rangle, \tag{A.3}
\end{aligned}$$

while

$$\begin{aligned}
\text{VAR}(\langle \beta, X \rangle) &= \mathbb{E}(\langle \beta, X \rangle^2) - (\mathbb{E}\langle \beta, X \rangle)^2 = \mathbb{E}(\langle \beta, X \rangle^2) - (\pi_D \langle \beta, \mu_D \rangle + \pi_H \langle \beta, \mu_H \rangle)^2 \\
&= \mathbb{E}\{\mathbb{E}(\langle \beta, X \rangle^2 | G)\} - (\pi_D \langle \beta, \mu_D \rangle + \pi_H \langle \beta, \mu_H \rangle)^2 \\
&= \{\pi_D \mathbb{E}(\langle \beta, X_D \rangle^2) + \pi_H \mathbb{E}(\langle \beta, X_H \rangle^2)\} - (\pi_D \langle \beta, \mu_D \rangle + \pi_H \langle \beta, \mu_H \rangle)^2 \\
&= \pi_D (\langle \beta, \Gamma_D \beta \rangle + \langle \beta, \mu_D \rangle^2) + \pi_H (\langle \beta, \Gamma_H \beta \rangle + \langle \beta, \mu_H \rangle^2) \\
&\quad - (\pi_D^2 \langle \beta, \mu_D \rangle^2 + \pi_H^2 \langle \beta, \mu_H \rangle^2 + 2\pi_D \pi_H \langle \beta, \mu_D \rangle \langle \beta, \mu_H \rangle) \\
&= \langle \beta, \Gamma_{\text{POOL}} \beta \rangle + \pi_D \pi_H \langle \beta, \mu_D \rangle^2 + \pi_D \pi_H \langle \beta, \mu_H \rangle^2 - 2\pi_D \pi_H \langle \beta, \mu_D \rangle \langle \beta, \mu_H \rangle.
\end{aligned}$$

Therefore,

$$\text{VAR}(\langle \beta, X \rangle) = \langle \beta, \Gamma_{\text{POOL}} \beta \rangle + \pi_D \pi_H \langle \beta, \mu_D - \mu_H \rangle^2,$$

which together with the fact that $\text{VAR}(G) = \pi_D \pi_H$ entails that

$$\text{corr}(\langle \beta, X \rangle, G) = \frac{\pi_D \pi_H \langle \beta, \mu_D - \mu_H \rangle}{\{\pi_D \pi_H (\langle \beta, \Gamma_{\text{POOL}} \beta \rangle + \pi_D \pi_H \langle \beta, \mu_D - \mu_H \rangle^2)\}^{1/2}} = \frac{\pi_D^{1/2} \pi_H^{1/2} L_{\text{POOL}}(\beta)}{\{1 + L_{\text{POOL}}^2(\beta)\}^{1/2}},$$

concluding the proof of a).

b) Follows immediately noting that $\Gamma_{\text{POOL}} = \Gamma$ when $\pi_D = 1/2$ or when $\Gamma_H = \Gamma_D$, since $\pi_D + \pi_H = 1$ and the analogy between maximizing the AUC which corresponds to maximizing

$L(\beta)$ and that of maximizing $\text{corr}(\langle \beta, X \rangle, Z)$, which corresponds to $L_{\text{POOL}}(\beta)$. ■

Proof of Proposition 3.2. Analogously to $\mathcal{R}(\Gamma)$, define

$$\mathcal{R}(\Gamma^{1/2}) = \left\{ y \in \mathcal{H} : \sum_{\ell \geq 1} \frac{1}{\lambda_\ell} \langle y, \phi_\ell \rangle^2 < \infty \right\},$$

and the inverse of $\Gamma^{1/2}$, which is well defined over $\mathcal{R}(\Gamma^{1/2})$, as

$$\Gamma^{-1/2}(y) = \sum_{\ell \geq 1} \frac{1}{\lambda_\ell^{1/2}} \langle y, \phi_\ell \rangle \phi_\ell.$$

The fact that $\lambda_\ell \rightarrow 0$ as $\ell \rightarrow \infty$ entails that for ℓ large enough $\lambda_\ell^2 < \lambda_\ell$, so taking into account that $\mu_D - \mu_H \in \mathcal{R}(\Gamma)$, we get that $\mu_D - \mu_H \in \mathcal{R}(\Gamma^{1/2})$.

Let $R = (\pi_D \pi_H)^{-1/2} \Gamma^{-1/2} \Gamma_{XG} : \mathbb{R} \rightarrow L^2(0, 1)$ with Γ_{XG} being the covariance operator between X and G , that is, the operator $\Gamma_{XG} : \mathbb{R} \rightarrow \mathcal{H}$ such that for any $a \in \mathbb{R}$, $\text{COV}(\langle u, X \rangle, aG) = \langle u, \Gamma_{XG}(a) \rangle$. Denoting $\gamma_{XG} = \Gamma_{XG}(1)$ we have that $\text{COV}(\langle u, X \rangle, G) = \langle u, \gamma_{XG} \rangle$. Analogous arguments to those considered in Theorem 4.8 of [He et al. \(2003\)](#) allow to show that the value β_0 maximizing $\text{corr}^2(\langle \beta, X \rangle, G)$ (respectively, the AUC) equals $\beta_0 = \Gamma^{-1/2} \psi_0$, where ψ_0 is the eigenfunction of the operator

$$R_0 = R R^* : L^2(0, 1) \rightarrow L^2(0, 1)$$

related to its largest eigenvalue and R^* stands for the adjoint operator of R .

From [\(A.3\)](#), we get that $\gamma_{XG} = \pi_D \pi_H (\mu_D - \mu_H)$, then if $\Delta_{DH} = (\pi_D \pi_H)^{1/2} \Gamma^{-1/2} (\mu_D - \mu_H) \in \mathcal{H}$, we get that $Ra = a \Delta_{DH}$ and $R_0 = \Delta_{DH} \{\Delta_{DH}\}^*$. Note that $R^* : L^2(0, 1) \rightarrow \mathbb{R}$ satisfies $\langle u, Ra \rangle = a R^* u$, for any $a \in \mathbb{R}$, $u \in L^2(0, 1)$, hence we have that

$$\langle u, Ra \rangle = a \langle u, \Delta_{DH} \rangle = a \int_0^1 \Delta_{DH}(t) u(t) dt,$$

and R^* is the linear operator with representative Δ_{DH} , i.e., $R^* u = \langle u, \Delta_{DH} \rangle$. Therefore, R_0 has only one eigenvalue different from 0, since for any $u \in \mathcal{H}$ orthogonal to Δ_{DH} , $R_0 u = 0$ and

$R^* \Delta_{DH} = \|\Delta_{DH}\|^2$ meaning that

$$R_0 \Delta_{DH} = R \|\Delta_{DH}\|^2 = \|\Delta_{DH}\|^2 \Delta_{DH}.$$

Thus, $\psi_0 = \Delta_{DH} / \|\Delta_{DH}\|$ and $\beta_0 = (\pi_D \pi_H)^{1/2} \Gamma^{-1} (\mu_D - \mu_H)$, concluding the proof. \blacksquare

Proof of Proposition 3.3. a) follows easily noting that $A^* A \alpha = \sum_{\ell=1}^k \langle \alpha, \phi_\ell \rangle \phi_\ell$, $\alpha^\top \mathbf{x} = \langle A \alpha, AX \rangle$ and the fact that

$$\Gamma_j^{-1} y = \sum_{\ell \geq 1} \frac{1}{\lambda_{j,\ell}} \langle y, \phi_\ell \rangle \phi_\ell, \quad \text{for any } y \in \mathcal{R}(\Gamma_j), \quad (\text{A.4})$$

which implies that $A \Gamma_j^{-1} \mu_j = \Sigma_j^{-1} \mu_j$.

b) Note that

$$\mathbf{x}^\top \Lambda \mathbf{x} = \sum_{\ell=1}^k \Lambda_\ell x_\ell^2 = \sum_{\ell=1}^k \Lambda_\ell \langle X, \phi_\ell \rangle^2 = \sum_{\ell=1}^k \frac{1}{\lambda_{D,\ell}} \langle X, \phi_\ell \rangle^2 - \sum_{\ell=1}^k \frac{1}{\lambda_{H,\ell}} \langle X, \phi_\ell \rangle^2.$$

Taking into account (A.4) and that from the definition of the linear operator A , we have that

$$A \Gamma_j^{-1} y = \left(\frac{\langle y, \phi_1 \rangle}{\lambda_{j,1}}, \dots, \frac{\langle y, \phi_k \rangle}{\lambda_{j,k}} \right)^\top,$$

we easily obtain that, for any $X \in \mathcal{R}(\Gamma_D^{1/2}) \cap \mathcal{R}(\Gamma_H^{1/2})$,

$$\sum_{\ell=1}^k \frac{1}{\lambda_{j,\ell}} \langle X, \phi_\ell \rangle^2 = \|A \Gamma_j^{-1} X\|^2.$$

The expression for $\Upsilon(X)$ follows easily from the convergence of the series $\sum_{\ell \geq 1} \langle X, \phi_\ell \rangle^2 / \lambda_{j,\ell}$, for $j = D, H$, and of the series $\sum_{\ell \geq 1} \langle \alpha, \phi_\ell \rangle \langle X, \phi_\ell \rangle = \langle \alpha, X \rangle$, concluding the proof. \blacksquare

8.3 Proof of the results in Section 4

Proof of Theorem 4.1. From Assumption **A3** and the continuity of the quantile function $F_H^{-1} = F_{H,\Upsilon}^{-1} : [0, 1] \rightarrow \mathbb{R}$ when Assumption **A1** holds, we get that for each $0 < p < 1$, $\widehat{F}_j^{-1}(p) - F_j^{-1}(p) \xrightarrow{a.s.} 0$. Therefore, using the continuity of F_D stated in Assumption **A2**, the uniform convergence required in Assumption **A3** for $j = D$ and the inequality

$$\begin{aligned} |\widehat{\text{ROC}}(p) - \text{ROC}(p)| &= \left| \widehat{F}_D \left\{ \widehat{F}_H^{-1}(1-p) \right\} - F_D \left\{ F_H^{-1}(1-p) \right\} \right| \\ &\leq \left| \widehat{F}_D \left\{ \widehat{F}_H^{-1}(1-p) \right\} - F_D \left\{ \widehat{F}_H^{-1}(1-p) \right\} \right| + \left| F_D \left\{ \widehat{F}_H^{-1}(1-p) \right\} - F_D \left\{ F_H^{-1}(1-p) \right\} \right| \\ &\leq \left\| \widehat{F}_D - F_D \right\|_\infty + \left| F_D \left\{ \widehat{F}_H^{-1}(1-p) \right\} - F_D \left\{ F_H^{-1}(1-p) \right\} \right|, \end{aligned}$$

we derive that $\widehat{\text{ROC}}(p) \xrightarrow{a.s.} \text{ROC}(p)$. Moreover, the uniform convergence is obtained from the monotonicity of $\widehat{\text{ROC}}$ and ROC and also from the continuity of ROC . \blacksquare

Proof of Theorem 4.2. From the monotonicity of \widehat{F}_j and F_j and also the continuity of F_j , it will be enough to prove that $\widehat{F}_j(t) - F_j(t) \xrightarrow{a.s.} 0$.

Fix $j = D$ or H . Define $\mathbb{L}_t^{(j)}(\boldsymbol{\beta}) = \mathbb{P}(\mathbf{x}_j^\top \boldsymbol{\beta} \leq t)$ for any $t \in \mathbb{R}$, then

$$\begin{aligned} \left| \widehat{F}_j(t) - F_j(t) \right| &\leq \left| \widehat{F}_{\widehat{\boldsymbol{\beta}},j}(t) - \mathbb{L}_t^{(j)}(\widehat{\boldsymbol{\beta}}) \right| + \left| \mathbb{L}_t^{(j)}(\widehat{\boldsymbol{\beta}}) - F_{\boldsymbol{\beta}_0,j}(t) \right| = \left| \widehat{F}_{\widehat{\boldsymbol{\beta}},j}(t) - F_{\widehat{\boldsymbol{\beta}},j}(t) \right| \\ &\quad + \left| F_{\widehat{\boldsymbol{\beta}},j}(t) - F_{\boldsymbol{\beta}_0,j}(t) \right|. \end{aligned}$$

It suffices to prove that

$$\sup_{t \in \mathbb{R}} \sup_{\boldsymbol{\beta} \in \mathbb{R}^k} \left| \widehat{F}_{\boldsymbol{\beta},j}(t) - F_{\boldsymbol{\beta},j}(t) \right| \xrightarrow{a.s.} 0 \quad (\text{A.5})$$

and

$$\left| F_{\widehat{\boldsymbol{\beta}},j}(t) - F_{\boldsymbol{\beta}_0,j}(t) \right| \xrightarrow{a.s.} 0. \quad (\text{A.6})$$

To derive (A.5), let us consider the family of functions

$$\mathcal{F} = \{h_{\boldsymbol{\beta},t}(\mathbf{x}) = \mathbb{I}_{\{\mathbf{x}^\top \boldsymbol{\beta} \leq t\}} \text{ for } (\boldsymbol{\beta}, t) \in \mathbb{R}^k \times \mathbb{R}\}.$$

Taking into account that $\{g(\mathbf{x}) = \mathbf{x}^\top \boldsymbol{\beta} - t; (\boldsymbol{\beta}, t) \in \mathbb{R}^k \times \mathbb{R}\}$ is a finite-dimensional space of functions with dimension $p+1$, from Lemmas 9.6 in Kosorok (2008) we get that \mathcal{F} is a VC-class with index at most $p+3$. Hence, applying Lemmas 9.8 and 9.9(iii) in Kosorok (2008), we get that the class of functions \mathcal{F} is a VC-class with index $V(\mathcal{F})$ smaller or equal than $p+3$. Note that the envelope of \mathcal{F} equals $F \equiv 1$. Hence, Theorem 2.6.7 in van der Vaart and Wellner (1996) entails that, there exists a universal constant K such that, for any measure Q

$$N\{\epsilon, \mathcal{F}, L_1(Q)\} \leq K V(\mathcal{F}) (16e)^{V(\mathcal{F})} \left(\frac{1}{\epsilon}\right)^{V(\mathcal{F})-1},$$

which together with Theorem 2.4.3 in van der Vaart and Wellner (1996) or Theorem 2.4 in Kosorok (2008), leads to

$$\sup_{h \in \mathcal{F}} |P_n h - P_j h| \xrightarrow{a.s.} 0,$$

where we have used the standard notation in empirical processes, i.e., $Ph = \mathbb{E}\{h(\mathbf{X})\}$ and $P_n h = (1/n) \sum_{i=1}^n h(\mathbf{x}_i)$. Hence, we have that

$$\sup_{t \in \mathbb{R}} \sup_{\boldsymbol{\beta} \in \mathbb{R}^k} \left| \widehat{F}_{\boldsymbol{\beta},j}(t) - F_{\boldsymbol{\beta},j}(t) \right| \xrightarrow{a.s.} 0,$$

which concludes the proof of (A.5).

It remains to prove (A.6). To strengthen the dependence on the sample size denote $\widehat{\boldsymbol{\beta}}_n = \widehat{\boldsymbol{\beta}}$, where $n = n_D + n_H$. Then, from the fact that $\widehat{\boldsymbol{\beta}} \xrightarrow{a.s.} \boldsymbol{\beta}_0$, there exists $\mathcal{N} \subset \Omega$ such that $\mathbb{P}(\mathcal{N}) = 0$ and for $\omega \notin \mathcal{N}$, $\widehat{\boldsymbol{\beta}}_n(\omega) \rightarrow \boldsymbol{\beta}_0$. Take $\omega \notin \mathcal{N}$, then for any $\mathbf{x} \in \mathbb{R}^k$, $\mathbf{x}^\top \widehat{\boldsymbol{\beta}}_n(\omega) \rightarrow \mathbf{x}^\top \boldsymbol{\beta}_0$. Hence, if $\mathbf{x}_j \sim P_j$, the random variable $Z_n = \mathbf{x}_j^\top \widehat{\boldsymbol{\beta}}_n(\omega)$ converges to $Z = \mathbf{x}_j^\top \boldsymbol{\beta}_0$ everywhere, so $F_{\widehat{\boldsymbol{\beta}}_n(\omega),j}(t) = \mathbb{P}(Z_n \leq t) \rightarrow \mathbb{P}(Z \leq t) = F_j(t)$, for any t . Using the fact that $F_j(t)$ is

non-decreasing and continuous, we conclude that, for any $\omega \notin \mathcal{N}$,

$$\left\| F_{\widehat{\beta}_n(\omega),j} - F_j \right\|_{\infty} \rightarrow 0,$$

concluding the proof of (A.6). ■

Proof of Theorem 4.3. The proof is similar to that of Theorem 4.2. Denote \mathcal{H}_k the linear space spanned by ϕ_1, \dots, ϕ_k , that is, $\mathcal{H}_k = \{\beta = \sum_{s=1}^k b_s \phi_s, \mathbf{b} = (b_1, \dots, b_k)^{\top} \in \mathbb{R}^k\}$.

Using that \widehat{F}_j and F_j are non-decreasing function and the continuity of F_j , it will be enough to show that $\widehat{F}_j(t) - F_j(t) \xrightarrow{a.s.} 0$. Fix $j = D$ or H and define $\mathbb{L}_t^{(j)}(\beta) = \mathbb{P}(\langle X_j, \beta \rangle \leq t)$, then

$$\begin{aligned} \left| \widehat{F}_j(t) - F_j(t) \right| &\leq \left| \widehat{F}_{\widehat{\beta},j}(t) - \mathbb{L}_t^{(j)}(\widehat{\beta}) \right| + \left| \mathbb{L}_t^{(j)}(\widehat{\beta}) - F_{\beta_0,j}(t) \right| = \left| \widehat{F}_{\widehat{\beta},j}(t) - \mathbb{L}_t^{(j)}(\widehat{\beta}) \right| \\ &\quad + \left| F_{\widehat{\beta},j}(t) - F_{\beta_0,j}(t) \right|. \end{aligned}$$

It is enough to show that

$$\sup_{t \in \mathbb{R}} \sup_{\beta \in \mathcal{H}_k} \left| \widehat{F}_{\beta,j}(t) - F_{\beta,j}(t) \right| \xrightarrow{a.s.} 0 \tag{A.7}$$

and

$$\left| F_{\widehat{\beta},j}(t) - F_{\beta_0,j}(t) \right| \xrightarrow{a.s.} 0. \tag{A.8}$$

The proof of (A.8) is similar to that of (A.6) and for that reason it is omitted.

To derive (A.7), we will follow similar arguments to those considered in the proof of Proposition 1 in Bianco and Boente (2023). Consider the family of functions

$$\mathcal{F} = \{h_{\beta,t}(x) = \mathbb{I}_{\{\langle x, \beta \rangle \leq t\}} \text{ for } (\beta, t) \in \mathcal{H}_k \times \mathbb{R}\}.$$

Taking into account that for $\beta \in \mathcal{H}_k$, $\langle x, \beta \rangle = \sum_{s=1}^k b_s \langle x, \phi_s \rangle = \mathbf{x}^{\top} \mathbf{b}$, where $\mathbf{x} = (\langle x, \phi_1 \rangle, \dots, \langle x, \phi_k \rangle)^{\top}$, we obtain that $\{g(x) = \langle x, \beta \rangle - t; (\beta, t) \in \mathcal{H}_k \times \mathbb{R}\}$ is a finite-dimensional space of functions

with dimension $k + 1$. Thus, from Lemma 9.6 in [Kosorok \(2008\)](#) we get that \mathcal{F} is a VC-class with index at most $k + 3$. Hence, applying Lemmas 9.8 and 9.9(iii) in [Kosorok \(2008\)](#), we conclude that the class of functions \mathcal{F} is a VC-class with index $V(\mathcal{F})$ smaller or equal than $k + 3$. Note that the envelope of \mathcal{F} equals $F \equiv 1$. Hence, Theorem 2.6.7 in [van der Vaart and Wellner \(1996\)](#) entails that there exists a universal constant K such that, for any measure Q

$$N \{ \epsilon, \mathcal{F}, L_1(Q) \} \leq K (k + 3) (16e)^{k+3} \left(\frac{1}{\epsilon} \right)^{k+2}. \quad (\text{A.9})$$

To show $\sup_{h \in \mathcal{F}} |P_{n_j} h - P_j h| \xrightarrow{a.s.} 0$, where $P_j h = \mathbb{E} \{ h(X_j) \}$ and $P_{n_j} h = (1/n_j) \sum_{i=1}^{n_j} h(X_{j,i})$, it will be enough to prove that

$$\frac{1}{n_j} \log N \{ \epsilon, \mathcal{F}, L_1(P_{n_j}) \} \xrightarrow{p} 0. \quad (\text{A.10})$$

From [\(A.9\)](#) we get that

$$\frac{1}{n_j} \log N \{ \epsilon, \mathcal{F}, L_1(P_{n_j}) \} \leq C \frac{k+2}{n_j} \log \left(\frac{1}{\epsilon} \right),$$

for some constant C . Thus, using that $k_n/n \rightarrow 0$, we obtain that

$$\sup_{t \in \mathbb{R}} \sup_{\beta \in \mathcal{H}^k} \left| \widehat{F}_{\beta,j}(t) - F_{\beta,j}(t) \right| \xrightarrow{a.s.} 0,$$

which concludes the proof of [\(A.7\)](#). ■

Proof of Theorem 4.4. Note that b) is a direct consequence of a) and [Theorem 4.1](#), so we will only show a). For that purpose recall that, for any $\boldsymbol{\alpha} \in \mathbb{R}^k$ and $\boldsymbol{\Lambda} \in \mathbb{R}^{k \times k}$, we have denoted $\Upsilon_{\boldsymbol{\Lambda}, \boldsymbol{\alpha}}(X) = -\mathbf{x}^\top \boldsymbol{\Lambda} \mathbf{x} + \boldsymbol{\alpha}^\top \mathbf{x}$ where $\mathbf{x} = A(X) = (\langle X, \phi_1 \rangle, \dots, \langle X, \phi_k \rangle)^\top$ and as in the proof of [Theorem 4.3](#) let $L_t^{(j)}(\boldsymbol{\Lambda}, \boldsymbol{\alpha}) = \mathbb{P}(\Upsilon_{\boldsymbol{\Lambda}, \boldsymbol{\alpha}}(X_j) \leq t)$. Then,

$$|\widehat{F}_j(t) - F_j(t)| \leq |\widehat{F}_j(t) - L_t^{(j)}(\widehat{\boldsymbol{\Lambda}}, \widehat{\boldsymbol{\alpha}})| + |L_t^{(j)}(\widehat{\boldsymbol{\Lambda}}, \widehat{\boldsymbol{\alpha}}) - L_t^{(j)}(\boldsymbol{\Lambda}_0, \boldsymbol{\alpha}_0)|. \quad (\text{A.11})$$

As in the proof of [\(A.6\)](#), the second term on the right hand side in [\(A.11\)](#) converges almost surely

to 0, since $(\widehat{\Lambda}, \widehat{\alpha}) \xrightarrow{a.s.} (\Lambda_0, \alpha_0)$. Hence, we only have to show that $\widehat{F}_j(t) - L_t^{(j)}(\widehat{\Lambda}, \widehat{\alpha}) \xrightarrow{a.s.} 0$, which follows as in Theorem 4.2 using that the class of functions

$$\mathcal{F} = \left\{ h_{\Lambda, \alpha, t}(X) = \mathbb{I}_{\{-\mathbf{x}^\top \Lambda \mathbf{x} + \alpha^\top \mathbf{x} \leq t\}}, \Lambda \in \mathbb{R}^{k \times k}, \alpha \in \mathbb{R}^k, t \in \mathbb{R}, \text{ where } \mathbf{x} = A(X) \right\},$$

is a finite-dimensional space of functions. ■

Acknowledgement

This research of A. M. Bianco and G. Boente was partially supported by Grants 20020170100022BA from the Universidad de Buenos Aires and PICT 2021-I-A-00260 from ANPCYT, Argentina. The three authors were also supported by Grants PID2020-118101GB-I00 (MCIN/AEI/10.13039/501100011033) and PID2023-148811NB-I00 (MICIU/AEI/10.13039/501100011033 and ERDF/EU), Spain. The research was begun while A. M. Bianco and G. Boente were visiting the Universidade de Vigo.

References

- Bali, J. L. and Boente, G. (2009). Principal points and elliptical distributions from the multivariate setting to the functional case. *Statistics and Probability Letters*, 79:1858–1865.
- Benko, M. and Härdle, W. (2005). Common functional implied volatility analysis. *In Statistical Tools for Finance and Insurance, Eds: Pavel Čížek, Rafal Weron and Wolfgang Härdle*, pages 115–134. Springer.
- Bianco, A. M. and Boente, G. (2023). Addressing robust estimation in covariate-specific ROC curves. *Econometrics and Statistics*. In press, available at <https://doi.org/10.1016/j.ecosta.2023.04.001>.
- Boente, G., Rodríguez, D., and Sued, M. (2010). Inference under functional proportional and common principal components models. *Journal of Multivariate Analysis*, 101:464–475.
- Boente, G., Salibián-Barrera, M., and Tyler, D. (2014). A characterization of elliptical distributions

- and some optimality properties of principal components for functional data. *Journal of Multivariate Analysis*, 131:254–264.
- Coffey, N., Harrison, A. J., Donaghue, O. A., and Hayes, K. (2011). Common functional principal components analysis: A new approach to analyzing human movement data. *Human Movement Science*, 30:1144–1166.
- Estévez-Pérez, G. and Vieu, P. (2021). A new way for ranking functional data with applications in diagnostic test. *Computational Statistics*, 36:127–154.
- Ferraty, F. and Vieu, P. (2006). *Nonparametric Functional Data Analysis: Theory and Practice*. Springer.
- Flury, B. (1984). Common principal components in k groups. *Journal of the American Statistical Association*, 79:892–898.
- Flury, B. (1988). *Common Principal Components and Related Multivariate Models*. Wiley.
- Flury, B. and Schmid, M. (1992). Quadratic discriminant functions with constraints on the covariances matrices: Some asymptotic results. *Journal of Multivariate Analysis*, 40:244–261.
- Frahm, G. (2004). *Generalized Elliptical Distributions: Theory and Applications*. PhD thesis, University of Köln, Germany.
- Haben, M., Tian, L., and Ghebremichael, M. (2019). The ROC curve for regularly measured longitudinal biomarkers. *Biostatistics*, 20:433–451.
- He, G., Müller, H., Wang, J., and Yang, W. (2003). Functional canonical analysis for square integrable stochastic processes. *Journal of Multivariate Analysis*, 85:54–77.
- Horváth, L. and Kokoszka, P. (2012). *Inference for Functional Data with Applications*. Springer.
- Hsing, T. and Eubank, R. (2015). *Theoretical foundations of Functional Data Analysis with an introduction to Linear Operators*, volume 997. John Wiley and Sons.
- Hult, H. and Lindskog, F. (2002). Multivariate extremes, aggregation and dependence in elliptical distributions. *Advances in Applied Probability*, 34:587–608.

- Inácio, V., González-Manteiga, W., Febrero-Bande, M., Gude, F., Alonzo, T., and Cadarso-Suárez, C. (2012). Extending induced ROC methodology to the functional context. *Biostatistics*, 13:594–608.
- Inácio de Carvalho, V., de Carvalho, M., Alonzo, T., and González-Manteiga, W. (2016). Functional covariate-adjusted partial area under the specificity-ROC curve with an application to metabolic syndrome diagnosis. *Annals of Applied Statistics*, 10:1472–1495.
- Jang, J. H. and Manatunga, A. (2022). Diagnostic evaluation of pharmacokinetic features of functional markers. *Journal of Biopharmaceutical Statistics*, 33:307–323.
- Kosorok, M. R. (2008). *Introduction to Empirical Processes and Semiparametric Inference*. Springer.
- Krzanowski, W. J. and Hand, D. J. (2009). *ROC Curves for Continuous Data*. Chapman and Hall.
- Leurgans, S. E., Moyeed, R. A., and Silverman, B. W. (1993). Canonical correlation analysis when the data are curves. *Journal of the Royal Society, Series B*, 55:725–740.
- Liu, H., Li, G., Cumberland, W., and Wu, T. (2005). Testing statistical significance of the area under a receiving operating characteristics curve for repeated measures design with bootstrapping. *Journal of Data Science*, 3:257–278.
- Liu, H. and Wu, T. (2003). Estimating the area under a receiver operating characteristic (ROC) curve for repeated measures design. *Journal of Statistical Software*, 8:1–18.
- Ma, S. and Huang, J. (2005). Regularized ROC method for disease classification and biomarker selection with microarray data. *Bioinformatics*, 21:4356–4362.
- Ma, S. and Huang, J. (2007). Combining multiple markers for classification using ROC. *Biometrics*, 63:751–757.
- Pepe, M. (2003). *The Statistical Evaluation of Medical Tests for Classification and Prediction*. Oxford University Press.
- Pepe, M., Cai, T., and Longton, G. (2006). Combining predictors for classification using the area under the Receiver Operating Characteristic Curve. *Biometrics*, 62:221–229.

- Pérez-Fernández, S. (2020). *ROC curves for multivariate markers*. PhD thesis, PhD. dissertation, Universidad de Oviedo and Technische Universität Wien (supervisors Corral Blanco, N., Martínez Cambor, P. and Filzmoser, P.).
- Piñeiro-Lamas, B., López-Cheda, A., Cao, R., Ramos-Alonso, L., González-Barbeito, G., Barbeito-Caamaño, C., and Bouzas-Mosquera, A. (2023). A cardiotoxicity dataset for breast cancer patients. *Scientific Data*, 10:527.
- Ramsay, J. and Silverman, B. (2005). *Functional Data Analysis, 2nd edition*. Springer.
- Sun, Y. and Genton, M. G. (2011). Functional boxplots. *Journal of Computational and Graphical Statistics*, 20:316–334.
- van der Vaart, A. W. and Wellner, J. A. (1996). *Weak Convergence and Empirical Processes*. Springer, New York.
- Wang, J. L., Chiou, J., and Müller, H. (2016). Functional data analysis. *Annual Review of Statistics and Its Application*, 3:257–295.
- Zhou, X. H., McClish, D. K., and Obuchowski, N. A. (2011). *Statistical Methods in Diagnostic Medicine*. John Wiley & Sons, New York.